



Norwegian University of
Science and Technology

Piston Pin Testing

Joakim Bøhn

Master of Science in Mechanical Engineering

Submission date: June 2016

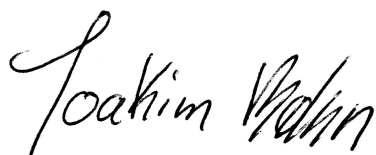
Supervisor: Terje Rølvåg, IPM

Norwegian University of Science and Technology
Department of Engineering Design and Materials

Preface

This master thesis was written in the subject TMM4901, Engineering Design, Calculation and Manufacture, at the Department of Engineering Design and Materials (NTNU), in the spring of 2016. This thesis used Siemens PLM software tool NX and Dassault Systemes Abaqus FEA to design and model a piston pin and perform finite element analysis.

I greatly appreciate my supervisor prof. Terje Rølvåg for his guidance and good advices during this project. A special thanks to Matteo Bella from MX Real Racing for being my contact person and answering all my questions.

A handwritten signature in black ink, reading "Joakim Bøhn". The signature is written in a cursive, flowing style.

Joakim Bøhn (Sign.)

Trondheim 10.06.2016

Abstract

This thesis addresses a study undertaken to develop a finite element model and perform quasi-static tests. The test is to simulate the piston and connecting rod execute a pressure force on the piston pin in a Honda CRF250F motorcycle. A variety of different piston pins are introduced to analyse how the mechanical strength of the pins is influenced depending on the change of their inner shape. By analysing the quasi-static tests conducted, an iterative process is performed to reduce the weight but maintaining the desired strength parameters at the same time.

Sammen drag

Denne avhandlingen tar for seg et studie for å utvikle en modell innenfor elementmetoden for å utøve kvasistatiske tester. Testen er for å simulere et stempel og råde utføre en trykkraft på stempelbolten i en Honda CRF250F motorsykkel. En rekke forskjellige stempelbolter innføres for å analysere hvordan den mekaniske styrken av stempelbolten blir påvirket avhengig av endringen av deres indre form. Ved å analysere kvasistatiske tester, en iterativ prosess utføres for å redusere vekten på bolten, men fortsatt opprettholde den ønskede styrkeparameteren.

Contents

Preface	i
Abstract	iii
Sammendrag	iii
List of Figures	x
List of Tables	xi
Abbreviations	xiii
1 Introduction	1
1.1 Background	1
1.2 Objective	2
2 Theory	3
2.1 Piston and Connecting Rod Assembly	3
2.2 Piston Pin	5
2.2.1 Circlips	6
2.2.2 Play	6
2.3 General Introduction to Abaqus FEA	7
2.3.1 Quasi-static Analysis	8
2.4 General introduction to Siemens NX	9

3	Relevant Publications on Piston Pins	11
3.1	Fessler and Hyde (1997)	11
3.2	Ramamurti et al. (2012)	12
3.3	Folega et al. (2015)	13
3.4	Wang and Gao (2011)	13
4	Physical Test	15
4.1	Results	16
5	Simulation of Physical Testing	19
5.1	Mesh	20
5.1.1	Hourglassing	21
5.1.2	Mesh Sensitivity Study	22
5.2	Analysis	23
5.3	Results	24
6	A New Simulation	27
6.1	Objective	27
6.2	A New Model	28
6.2.1	Mesh	30
6.2.2	Mesh Sensitivity Study	30
6.2.3	Geometry	32
7	Optimisation, Results and Discussion	33
7.1	Path Selection	33
7.2	OEM	35
7.3	True Hole Piston Pin	38
7.4	Design Proposals	40
7.5	Further Iteration	42
7.6	Discussion	45
7.7	Final Design	47
7.8	Play Analysis	50

<i>CONTENTS</i>	vii
7.9 Machining	51
8 Summary	53
8.1 Further Work	53
8.2 Conclusion	54
Bibliography	59
A	I
A.1 Light Weight Metals	I
A.2 Ceramics	III
B OEM Machine Drawing	V
C Final Design Machine Drawing	VII
D Master Assignment	IX
E Risikovurdering	XI

List of Figures

2.1	Piston pin load illustration. (Heiserman, 2015)	3
2.2	Four-stroke cycle. (WordPress, 2015)	4
2.3	Piston pin applied load illustration	5
2.4	Abaqus analysis phases (Dassault Systèmes, 2013)	7
2.5	Quasi-static analogy (Dassault Systèmes, 2014)	8
3.1	Case 1 and case 2 (Ramamurti et al., 2012)	13
4.1	Physical test used in a similar experiment. (May et al., 2008)	15
4.2	Test tools	16
4.3	Various design profiles	17
4.4	Test results	17
5.1	Abaqus model	20
5.2	Different hex elements (“Element Selection Criteria,” n.d.)	21
5.3	Master slave surface penetration (Dassault Systèmes, 2013)	21
5.4	Hourglassing. (“Optimec Consultants”, n.d.)	22
5.5	Hourglassing post-processing visualisation	22
5.6	Mesh sensitivity study	23
5.7	Abaqus material input	24
5.8	OEM force vs displacement	25
5.9	Simulation force vs displacement	26
5.10	Physical testing and simulation results	26

6.1	Piston assembly	29
6.2	The new Abaqus model	30
6.3	Mesh sensitivity study	31
6.4	Abaqus model for play study	32
7.1	Von Mises path OEM	34
7.2	OEM displacement paths	34
7.3	Von Mises stress OEM piston pin	36
7.4	Displacement OEM piston pin	37
7.5	Von Mises stress	39
7.6	Displacement	39
7.7	Various design proposals	40
7.8	Masses	41
7.9	Von Mises stress	41
7.10	Displacement	42
7.11	Masses	43
7.12	Von Mises stress	43
7.13	Displacement	44
7.14	Von Mises stress path	44
7.15	Displacement old simulation	46
7.16	Displacement new simulation	46
7.17	Further design proposals	47
7.18	Force vs displacement	48
7.19	Final design	49
7.20	Final design stress vs OEM stress	49
7.21	Final design displacement vs OEM displacement	50
7.22	Iscar tool (a) and sketch of the internal profiling (b). (ISCAR LTD., 2016)	52
7.23	Iscar PICCOCUT tool dimensions (ISCAR LTD., 2016)	52

List of Tables

5.1	Material properties	24
7.1	Iscar PICCOCUT tool dimensions (ISCAR LTD., 2016)	52

Abbreviations

NTNU Norwegian University Of Science and Technology

MXRR MX Real Racing

CAD Computer-aided design

FE Finite element

T.D.C. Top dead center

B.D.C. Bottom dead center

FEA Finite element analysis

CAE Complete Abaqus environment or Computer-aided engineering

CAM Computer-aided manufacturing

OEM Original equipment manufacturer

STA Solution treatment and aging

IGES Initial graphics exchange specification

DLC Diamond-like carbon

Chapter 1

Introduction

1.1 Background

In the last decades, high performance racing have had the need for reducing weight to affect fuel consumption, service life and performance. As a result, one strives to reduce the weight of its components as much as possible, and still maintaining the desired strength parameters at the same time. A beneficial way to do this is to trim the mass of moving parts in the internal combustion engines crucial sections, such as the crank system.

The piston pin, also known as a gudgeon pin or a wrist pin, is a central part of the crank system along with the piston and connecting rod. An optimisation of the piston pin in regards to design and choice of material can have a major impact. A classification between different piston pin designs and a variety of materials, leads to a number of approaches for the optimised piston pin. In commercial use, the common steel material is used for its strength and durability. In high performance racing, these characteristics are wanted, but with the lightweight property of materials such as titanium.

This thesis is a collaboration between the Norwegian University of Science and Technology (NTNU) and MX Real Racing (MXRR) in Italy. MXRR developed recently a test rig for physical testing of piston pins. Testing was conducted on

piston pins with various designs and material properties.

1.2 Objective

The objective is to identify the optimal combination of piston pin shape and material.

To make this objective a reality, a computer-aided design (CAD) of the physical testing simulation done by MXRR along with the various piston pin designs will be modelled using the Siemens NX software. This model will be imported into Abaqus and a quasi-static FE (Finite element) analysis is to be conducted. With an iterative process to adjust the material data used in the Abaqus analysis, the simulation is to give the same results as the physical testing. As a result of this, the material data will be obtained. Additionally an iterative process will be done until a more optimal piston pin design is obtained.

The main task is therefore to construct a realistic FE simulation of the physical test, so MXRR can use the model to refine its piston pin designs. The FE model is therefore to be used as an approve or disapprove filtration process before producing the piston pins and performing physical testing. In addition to this, a recommended piston design is proposed by an iterative process.

Chapter 2

Theory

2.1 Piston and Connecting Rod Assembly

The piston pin is a part in the internal combustion engine. It is connected to the piston and the connecting rod in the crank mechanism, as shown in figure 2.1. The piston pin fits into the small end of the connecting rod and is supported by the pin bosses on either side.

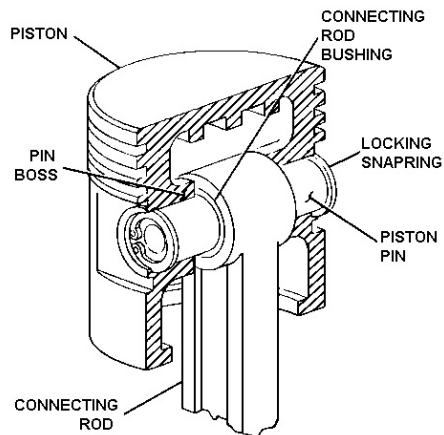


Figure 2.1: Piston pin load illustration. (Heiserman, 2015)

The Honda CRF250R have a four-stroke gasoline engine. The four strokes are termed:

- (a) Intake: Air and fuel enter the cylinder. The cycle goes from when the piston is at top dead center (T.D.C.) and ends when it is at bottom dead center (B.D.C.).
- (b) Compression: The piston goes from B.D.C. to T.D.C. and compress the air-fuel mixture.
- (c) Power: When the piston is at T.D.C. the air-fuel mixture is ignited by a spark plug and forces the piston to B.D.C.
- (d) Exhaust: The piston moves toward T.D.C. again and pushes the exhaust out of the combustion chamber.

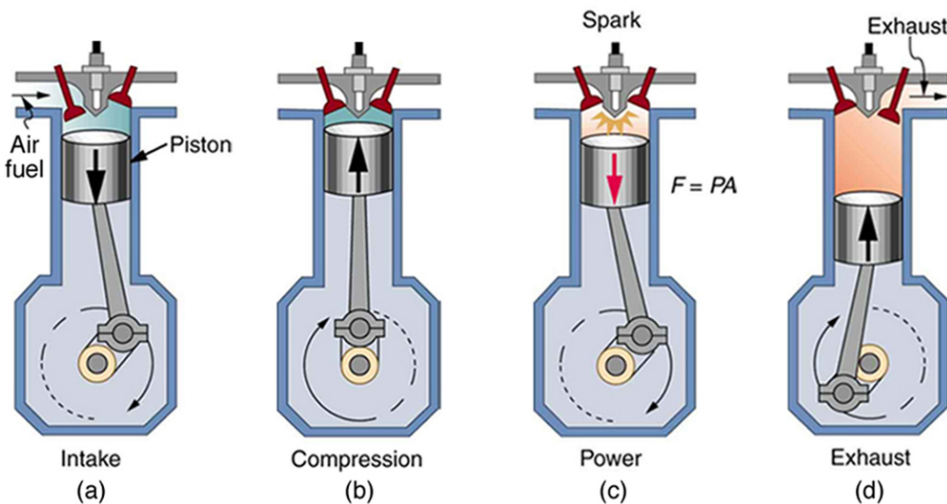


Figure 2.2: Four-stroke cycle. (WordPress, 2015)

During these cycles the piston goes up and down continuously. The crank mechanism consist of mainly the piston, piston pin and connecting rod. The mechanisms function is to convert reciprocating motion due to the pressure exerted on the piston surface, into circular motion as visualised in figure 2.2. The highest pressure inside the combustion chamber occurs during the power stroke. The instant the

air-fuel mixture ignites, a high force will exert on the piston surface and to the piston pin. As Michael Giannone, the founder of MGP connecting rod said “Most people don’t realize that during the firing cycle of one cylinder the piston pin carries the weight- the mass and momentum- of the whole car and drives it forward,” Giannone (2016)

2.2 Piston Pin

The main reason for pins fatigue failure is incorrect design (Ji et al., 2012). The piston pin is a crucial part in the engine. A pin failure will most definite lead to an irreparable engine. The conditions for the pin are hard and includes factors such as: high temperatures, high frequent forces, tight spacing and small sizing. All of which makes calculations challenging. At the stage of ignition in the engine, the force acting on the piston pin is illustrated in figure 2.3. This shows the pressure force onto the piston crown surface and the force on the connecting rod.

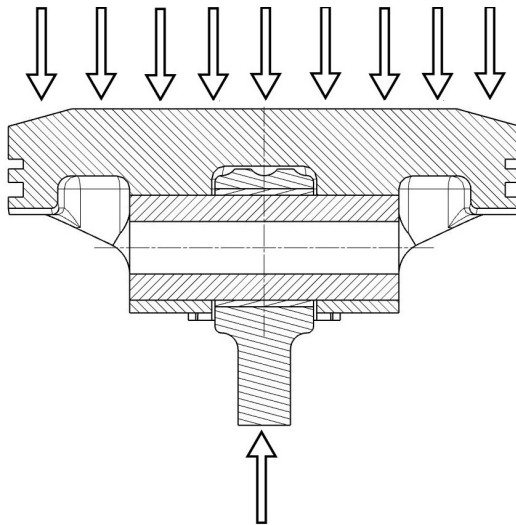


Figure 2.3: Piston pin applied load illustration

2.2.1 Circlips

A way to securely fasten the piston pin is by inserting circlips, also known as snap rings, at either end in the piston boss as shown in figure 2.1. If the piston pin were to slide out of its position it would scuff and wear the cylinder wall (Piston, 2016). Some piston pin manufactures do not make pins shorter than the length from the piston wall to the piston boss on the opposite side. If for some reason one of the pin clips came out, the pin can move to one side until it hits the cylinder wall and still be supported by both piston bosses.

2.2.2 Play

Another important feature regarding the fastening of the piston pin is the interference fit of the piston pin. Interference fit is a mechanical term for fastening between two parts. These two mating parts have a slightly deviating size from the nominal dimension. When pushed together by force, the friction between the two parts are too high for the parts to be separated by natural causes.

In the piston assembly, interference fit can be a way to secure the position of the piston pin without using circlips. This is explained as three different terms: stationary-, semi-floating- or fully-floating piston pin. (Shi, 2011; Abed et al., 2013)

- The stationary pin have an interference fit in the piston bosses and is free to rotate in the connecting rod. This is also known as a fixed pin.
- The semi-floating pin is secured to the connecting rod and free to move in the piston.
- The fully-floating pin are free to rotate in both the piston bosses and the connecting rod.

The level of floating, or empty space, between the pin and piston or connecting rod is known as “play”.

2.3 General Introduction to Abaqus FEA

Abaqus FEA is general-purpose simulation tool and can solve a wide range of engineering problems. The program offers three main products, Abaqus/Standard, Abaqus/Explicit and Abaqus/CAE (Dassault Systèmes, 2014). The standard and explicit products are analysis program for solving linear, nonlinear, static and dynamic problems. CAE is an acronym for “**C**omplete **A**baqus **E**nvironment” and is the graphical environment for pre and post-processing in Abaqus. A complete analysis consists of three distinct phases: Pre-processing, simulation and post-processing. This is shown in figure 2.4.

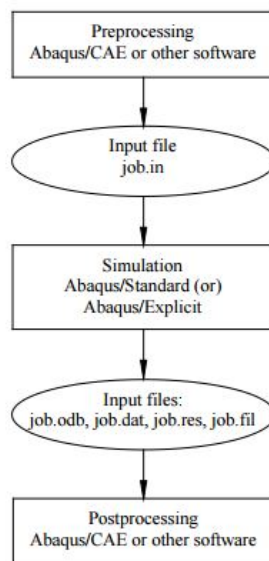


Figure 2.4: Abaqus analysis phases (Dassault Systèmes, 2013)

2.3.1 Quasi-static Analysis

Quasi-static loading analysis consider inertial effects as negligible. The Abaqus documentation use an analogy of a quasi-static case where a person walks into a crowded elevator, as shown in figure 2.5 (Dassault Systèmes, 2014). In the slow case, which is to simulate the quasi-static loading, the occupants adjacent to the door pushes the nearby individuals and so forth. This wave passes through the elevator until everyone reaches a new equilibrium position. In the fast case, which is to simulate a fast dynamic loading, the door opens and the person runs into the elevator so the occupants adjacent to the door have no time to rearrange themselves to accommodate. The individuals closest to the door will be injured while the nearby people will be unaffected.

A quasi-static load is therefore when the load is applied to an object in a very slow velocity and the structure deforms accordingly slowly. There is therefore a very low strain rate and therefore the inertia forces is very small and can be ignored.

As mentioned, Abaqus offers two different solvers, standard and explicit. The standard is also known as the implicit solver because it uses an implicit integration scheme. The implicit solver solves for true static equilibrium whereas the explicit solver solves for true dynamic equilibrium. To not go beyond the scope of this thesis a recommendation is that implicit solver would be appropriate for modelling highly nonlinear static problems. However, the explicit solver is to recommend for three-dimensional problems involving contact and very large deformations.

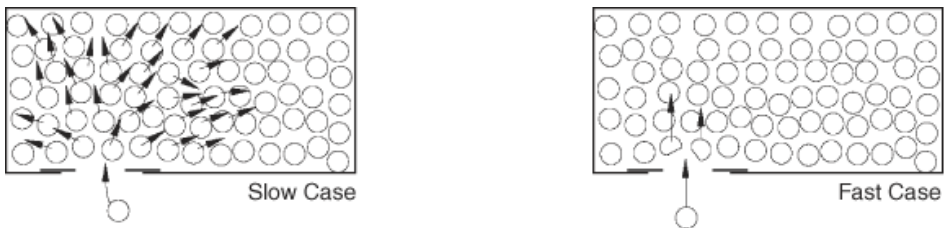


Figure 2.5: Quasi-static analogy (Dassault Systèmes, 2014)

2.4 General introduction to Siemens NX

NX is an advanced CAD/CAM/CAE software package originally developed by Unigraphics and first released in 2002 (Siemens PLM Software Inc., 2016). In 2007, Unigraphics were amalgamated into the Siemens PLM Software, a business unit of Siemens AG. The software offers three key functions:

Computer-aided design (CAD) - The design feature of the software. It offers parametric and direct modelling.

Computer-aided engineering (CAE) - The simulation feature of the software. It offers a wide range of engineering analysis using the finite element method.

Computer-aided manufacturing (CAM) - The manufacturing feature of the software. It offers software solutions for machine tool programming, post-processing and machining simulation.

Chapter 3

Relevant Publications on Piston Pins

Even though a lot of literature has played an important role of writing this thesis, a few texts are important to make a special note of. This is to describe what has been done before, and to further understand the results presented later. A brief summary of these are introduced in this chapter.

3.1 Fessler and Hyde (1997)

Fessler and Hyde did frozen stress photoelastic tests on four shapes of gudgeon pins loaded in a piston of realistic shape with a realistic connecting rod. They analysed the distributions of the pressures exerted on the pin using the flexibilities of the three components, piston, piston pin and connecting rod and the clearance between them as the variables. The article builds on previous work on calculations for bending stresses and shear stresses on piston pins. Rothmann (1963) proposed a method for calculating axial bending stresses. The piston pin was considered as a beam subjected to a uniformly distributed load along the length of the connecting rod and simply supported at the inner edges of the piston bosses, i.e. he calculated

the bending stresses in the pin according to simple beam theory. A similar approach was done by Schlaefke (1940). Instead of calculating with the simple support at the inner edges of the piston bosses, he considered the simple support to act a distance of approximately the equivalent of one quarter of the outside diameter of the pin from the end faces of the connecting rod. Under loading the circular cross-section became oval and the stresses were calculated by using ring theory. Dixon (1960) carried out tests on three pins loaded in an actual piston. The results he presented indicated that a hollow piston pin cannot be considered as a simple beam. Dixon found large shear stresses at the gap between the piston and connecting rod. Fessler and Padgham (1966) did a concentrated study on the results of Dixon. An important result from this study was that the reduction of the length of unsupported pin is more important than the greater flexibility of the bosses in piston and connecting rod.

The conclusion of Fessler and Hyde is an agreement with Dixon and Fessler and Padgham regarding that articles that use simple supported beam theory are misleading. The article suggest that even if the piston pin is replaced by two lugs in the gap between piston and connecting rod, it would change the stress picture in only a small amount.

3.2 Ramamurti et al. (2012)

Ramamurti et al. (2012) wrote an article regarding the deformation and stress on the piston pin in a reciprocating compressor used in air brake systems. A case study of play, see section 2.2.2, was conducted and compared with the inadequacy of the beam approach. An important discussion in this article is the relevance of play between the piston boss and piston pin during maximum displacement. The article presents a different in results when the piston pin is in contact with point B1 and B2, or when the piston pin is in contact with point A1, B1, B2 and A2 (figure 3.1).

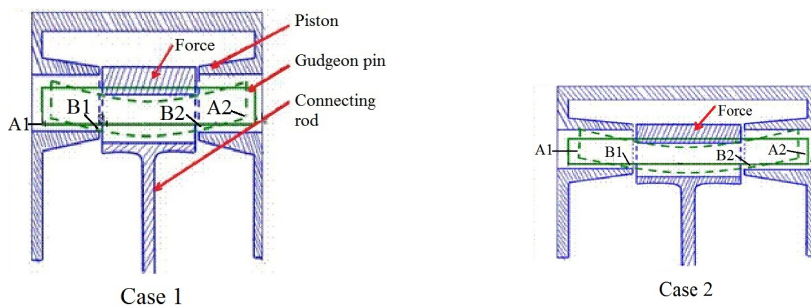


Figure 3.1: Case 1 and case 2 (Ramamurti et al., 2012)

3.3 Fołęga et al. (2015)

This article analyse how the piston pin inner design affected the stresses in the pin. For the purpose of calculations, various scenarios of the inner shape modifications were proposed. By using the Femap Siemens PLM software to conduct the numerical calculations, Fołęga et al. deliberate the various design benefits.

3.4 Wang and Gao (2011)

Wang and Gao performed an optimisation for the piston pin and the piston pin boss. By using FE analysis they conclude that the greatest stress concentration is caused on the upper end of the piston pin boss. When the stiffness of the piston is not enough, a crack will appear at this stress point and may cause splitting along the piston in a vertical direction. The stress distribution on the piston pin seat mainly depends on the deformation of the piston pin. By using beam bending- and elliptical deformation an optimisation algorithm is carried out using GA Toolbox in MATLAB software. The result is an optimised piston pin and piston pin boss with reduced maximum stress and a lower deformation.

Chapter 4

Physical Test

MXRR in Italy designed and manufactured tools to test piston pins in a hydraulic press machine, similar to the one presented in figure 4.1. The tools used for the test is shown in figure 4.2. The part on the left is to simulate the connecting rod-, and the part on the right the piston. The tools manufactured by MXRR is constructed in C40 steel. The purpose of the test is to validate new designs of piston pins in regards to force applied versus displacement of the piston pin.



Figure 4.1: Physical test used in a similar experiment. (May et al., 2008)

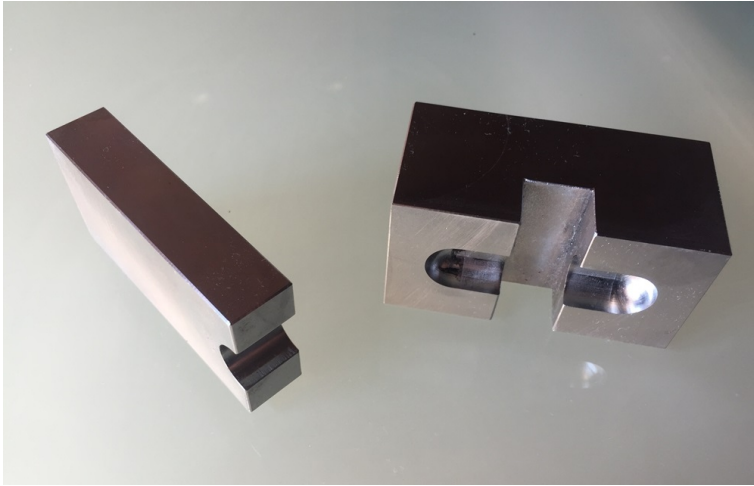


Figure 4.2: Test tools

4.1 Results

MXRR manufactured 4 different piston pins to be tested along with the original equipment manufacturer (OEM) piston pin. Honda do not release the material data they use for their engine components to the public. The exact material Honda uses for the piston pin is therefore unknown. It is still considered to behave equivalent to 4340 steel. The four different piston pins tested is shown in figure 4.3. The names of the piston pin is as follows:

OEM - This is the **O**riginal **E**quipment **M**anufacturer.

HGTi - This pin is made out of **H**igh **G**rade **T**itanium.

HGTi+STA - This pin is made out of **H**igh **G**rade **T**itanium and have the same design as the HGTi piston pin. In addition, this piston pin has been subjected to a **S**olution **T**reatment and **A**ging (STA) process to increase strength properties (Gupta et al., 2016).

Steel 1 - This piston pin is made out of **S**teel

Steel 2 - This piston pin is made out of **S**teel

The results of the test are shown in figure 4.4. The pressure during the power stroke in the engine of the motorcycle is equivalent to 6190N of force. As seen the different design and material properties gives a range of different deformation when subjected to this load. Between the piston pins made out of steel there are a deformation gap of over 7.5 percent. When accounting with the titanium pins there are a deformation gap of 42 percent. This shows that there are a lot of room for improvement.

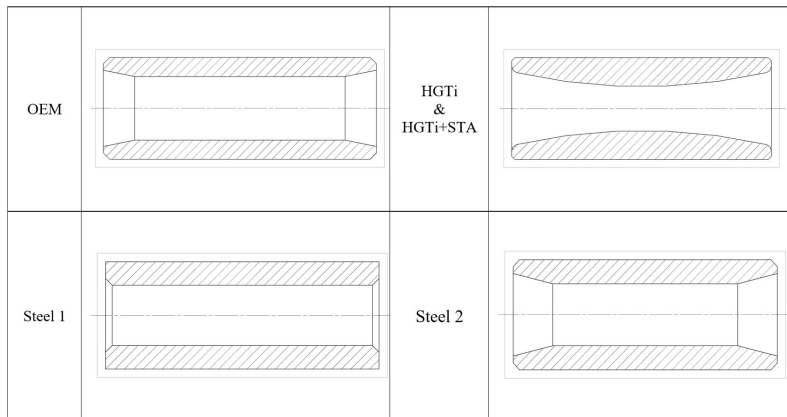


Figure 4.3: Various design profiles

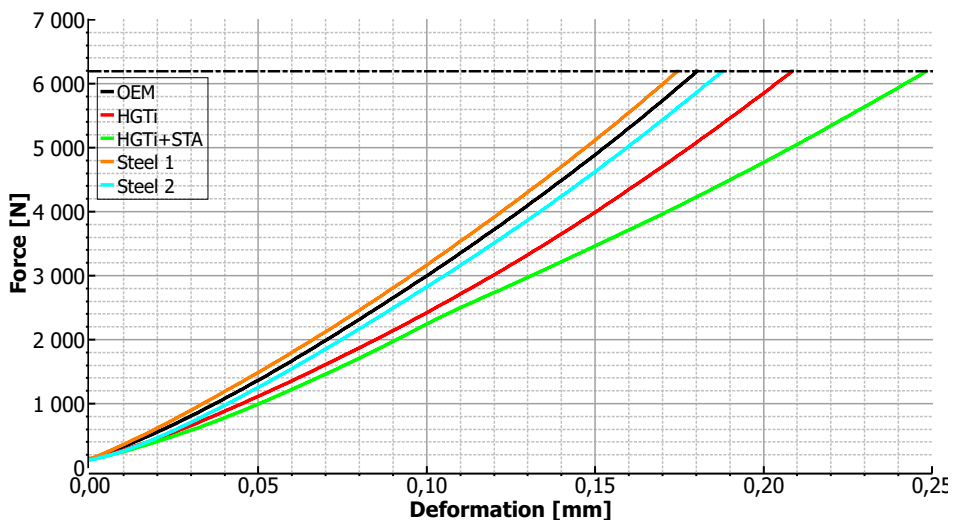


Figure 4.4: Test results

Chapter 5

Simulation of Physical Testing

An Abaqus model of the physical test was constructed. Due to a fairly big model and an excessive number of elements needed for a precise analysis of the test, some partitions of the test tools have been removed in order to save computing time and still give a precise results. The Abaqus model is shown in figure 5.1. The top part is to simulate the piston, and the bottom part the connecting rod. This solid 3-D FEA of the physical test is carried out by using the Abaqus 6.14-1 software. In order to obtain accurate results of this quasi-static analysis, surface-surface contact is applied to the model and a careful consideration of mesh is performed.

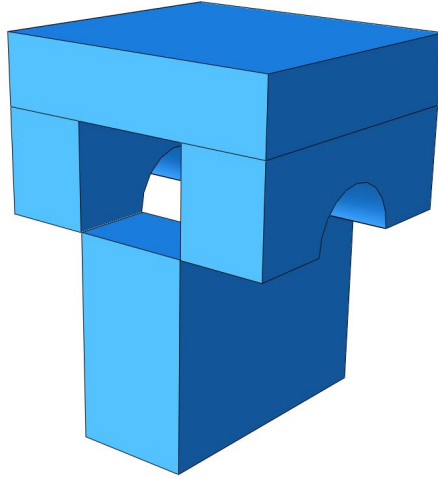


Figure 5.1: Abaqus model

5.1 Mesh

It is critical for the simulation to choose the right mesh and validate the mesh for the model. The different mesh elements Abaqus has to offer provides flexibility in modelling different geometries and structures. Each element family and the variation within each family gives a variety of different benefits for different analysis. During this analysis, elements with an accurate displacement calculation and surface-surface contact is needed. For this model, hexahedral solid elements is therefore used.

For solid hexahedral elements, one differs between first order interpolation and second order interpolation elements. The difference between the two is presented in figure 5.2. As seen, the first order interpolation elements have fewer integration nodes. This results in a geometric shape function difference. The first order interpolation will have a linear deformation ($Ax+B$), whereas the second order interpolation will have a quadratic function deformation (Ax^2+Bx+C). It is not recommended to use both in this simulation at the risk of penetration, see figure 5.3. This is a possibility if the master surface have a denser node distance then the slave surface. As seen in figure 5.2 it is possible to use elements with reduced

integration elements. This is an integration rule that is one order less than the full integration rule and will reduce the solution time of the analysis. The downside with reduced integration is the potential of hourglassing.

	Full integration	Reduced integration
First-order interpolation		
Second-order interpolation		

Figure 5.2: Different hex elements (“Element Selection Criteria,” n.d.)



Figure 5.3: Master slave surface penetration (Dassault Systèmes, 2013)

5.1.1 Hourglassing

Hourglassing is a spurious deformation mode of a FE mesh (Dassault Systèmes, 2013). The elements are severely deformed while the elements integration point are zero. A case of this is presented in figure 5.4. This is a pitfall with reduced integration elements. An example of hourglassing in the post-processing visualization in Abaqus is shown in figure 5.5. This is an example for the 8-node brick. This phenomena will give false results. Given the second-order interpolation for the 20-node brick, hourglassing is more rare and can be harder to diagnose visually in Abaqus. The most reliable diagnosis of hourglassing is by verifying that the

artificial energy of the simulation in abaqus is small ($<1\%$) relative to the internal energy. Due to a more accurate result and a smaller chance for hourglassing the mesh chosen for the model is the 20-node brick element with a reduced integration, which is known in Abaqus terms as C3D20R.

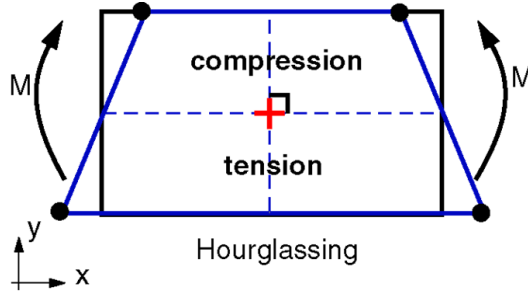


Figure 5.4: Hourglassing. (“Optimec Consultants”, n.d.)

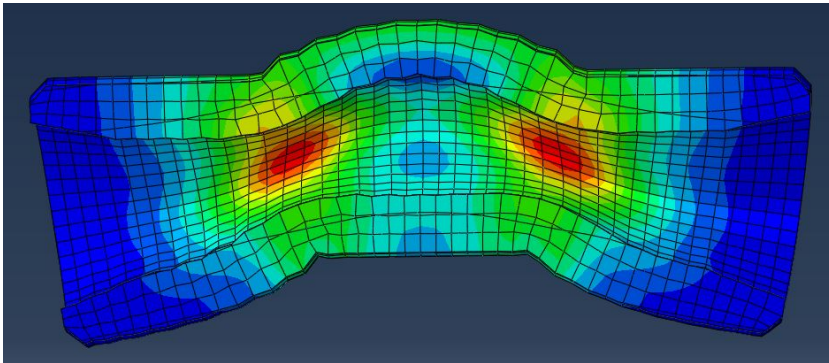


Figure 5.5: Hourglassing post-processing visualisation

5.1.2 Mesh Sensitivity Study

A high-density mesh will produce results with high accuracy. A mesh sensitivity study will give an idea of how many C3D20R elements is needed in the model to give accurate results and as few elements as possible to save the amount of computer memory and long run times. The result of this study is shown in figure 5.6. This study uses the maximum Von Mises stress as the parameter on the OEM piston pin. With a number of elements under 53000 the results vary because of too

few elements. The result for the study is that this model will use 75632 elements when included the OEM piston pin.

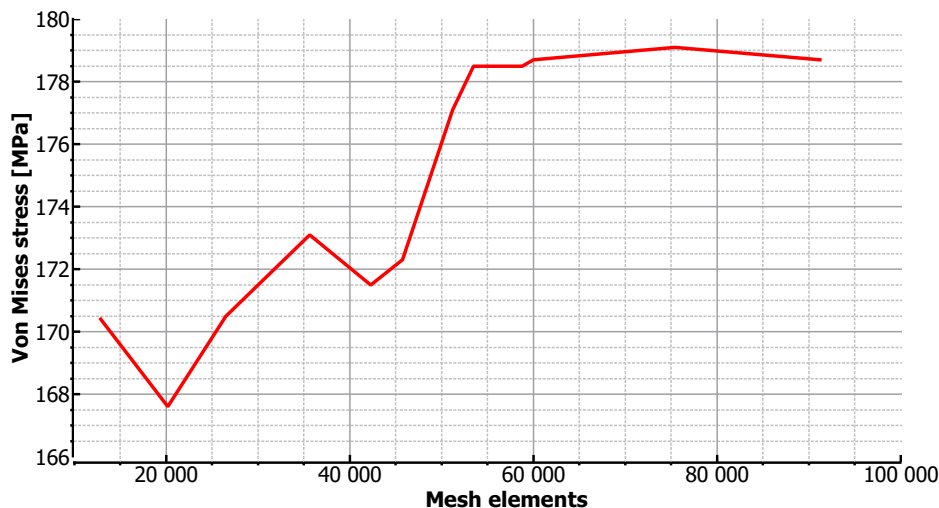


Figure 5.6: Mesh sensitivity study

5.2 Analysis

With the model complete, the analysis of the different piston pin designs and materials can be performed. The piston pins are designed in Siemens NX software, and imported to Abaqus in an IGES (Initial graphics exchange specification) format. Because of NX's friendly user interface with regards to design, this is the preferable method. As mentioned in the introduction of chapter 6, the parts to simulate the piston and the connecting rod in the physical test is manufactured with C40 steel. The iteration process starts with material data associated with these materials. The material data is shown in table 5.1. The material data is inserted in Abaqus as a bilinear material model. The characteristics of the plasticity in material model is not relevant because the pin shall never pass the point of yield. If the piston pin passes the yield strength of the material, only an indication that this occurs is interesting in this analysis. The friction coefficient is given from MXRR. Between the steel parts the coefficient is 0.8 and between the titanium pin and the steel 0.3.

Table 5.1: Material properties

	C40	4340 Steel	Ti Gr5 4928
Density [kg/m^3]	7850	7850	4430
Youngs modulus [GPa]	210	210	114
Poisson ratio [mm/mm]	0.3	0.3	0.3
Yield strength [MPa]	320	470	935
Ultimate tensile strength [MPa]	560	745	1000

In Abaqus these material properties reads the inputs as shown in figure 5.7 for the example of the 4340 steel alloy.

```
*Density
7.85e-09,
*Elastic
210000., 0.3
*Plastic
470., 0.
745., 0.28
```

Figure 5.7: Abaqus material input

5.3 Results

When the results were analysed, there were unexpected findings. The first result from the OEM design with 4340 steel properties is shown in figure 5.8. This shows a much stiffer piston pin with a tenth of a displacement in regards to the displacement measured in the experimental testbench. There were expected to be an iteration process to match the Abaqus material data with the material data from the physical test. Another peculiar finding in these result is that since the Abaqus material model at this stage have not been assigned material strengthen properties such as tempering and hardening of the material, it was suspected that the material data in Abaqus would be iterated to be stronger, not softer.

The other piston pin designs were imported to the model an analysed. Similar

result was presented. The results from all the different piston pins is shown in figure 5.9. To visualize the difference, figure 5.10 shows the experiment results and simulation results in the same graph. The similarity of graphs is that they both show a concave upward line. The reason for this is since the tools to simulate the piston and connecting rod in the physical test have a radius of 8.01, while the piston pin have a radius of 8.00. When the pressure exerts on the pin, it will have an elliptical deformation and the pin will gradually have more contact with the connecting rod and the piston.

As a consequence of these results there is no confident in extracting material data from this simulation. No fellow students or professors with experience with Abaqus at NTNU can't find anything wrong in the simulation. The physical testing is outsourced so the author of this thesis cannot perform additional troubleshooting with the physical test. For these reasons, it is hard to identify a reason for this error.

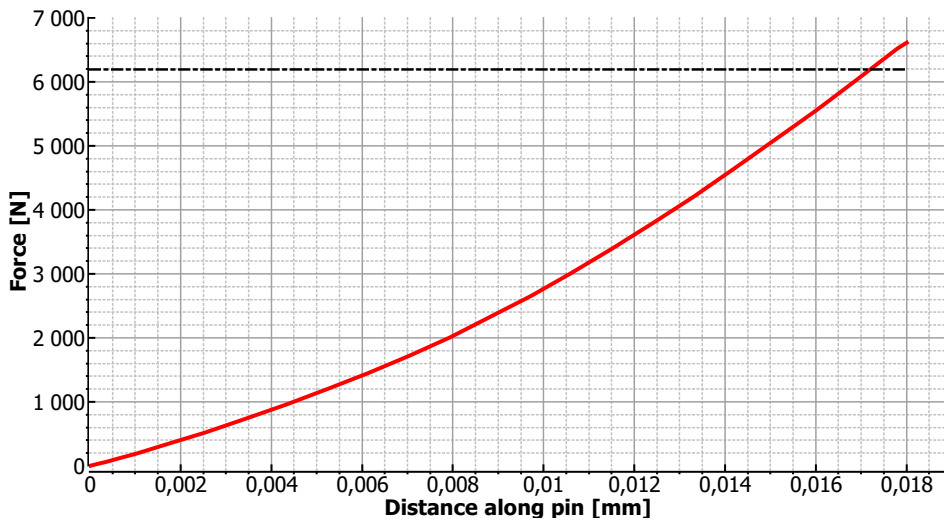


Figure 5.8: OEM force vs displacement

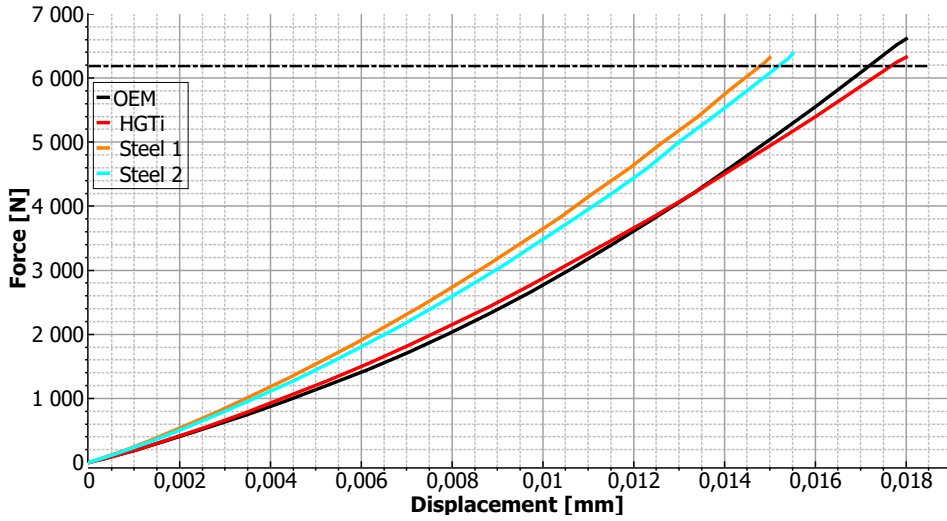


Figure 5.9: Simulation force vs displacement

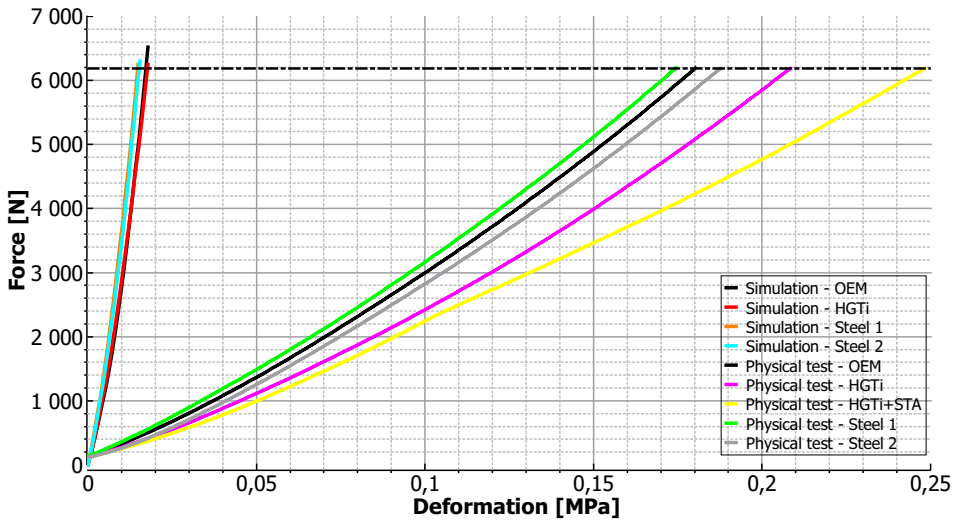


Figure 5.10: Physical testing and simulation results

Chapter 6

A New Simulation

After the previous results, a reassessment of the thesis was performed. Without the material data needed, not all the objectives set in section 1.2 could be executed and new objectives had to be made.

6.1 Objective

The focus is still on the Honda CRF250R motorcycle piston pin. The new objective will be to generate a new Abaqus FE model on the basis of the known parameters of the real life motorcycle assembly described in 2.1, and present an optimal piston pin design.

Proposals of new pin shapes will be introduced. It will be an iterative process, by using quasi-static analysis, until the optimal design is obtained. Every time a change is made, it has to be analysed again to see if the performance is enhanced or there are issues that have not been taken into account. All constrains and boundary conditions used in the previous simulation have to be revised, in order to make sure the simulation is as realistic as possible.

6.2 A New Model

Important topics in consideration of designing the new FE model:

- Piston geometry and material
- Connecting rod geometry and material.
- Play between piston pin and piston
- Play between piston pin and connecting rod.
- Real life environment boundaries of the piston pin.
- How can it be benchmarked?

Figure 6.1 shows the piston and connecting rod assembly in Abaqus. The arrows on the piston crown surface is to simulate the pressure load in the combustion chamber onto the piston. The connecting rod is constrained in all directions. Because of the excessive size of the model, this would need to be simplified. The OEM Honda CRF250R piston is made out of molded aluminium alloy and the connecting rod in steel. As mentioned, the material data is not shared from Honda. As a result of this, the material data assigned in Abaqus will always be an uncertainty.

A way to both eliminate the material uncertainty of the piston and connecting rod and preserve the geometry of the assembly is to use the geometry of these parts and create rigid parts in the Abaqus model, i.e. they resist deformation in response to an applied force. This proposed model is shown in figure 6.2. The pressure load on the piston crown assembly is exchanged with a pressure force tied to the piston bosses, and the connecting rod is constrained in all directions. This model uses just the piston pin as a solid part, with shell parts to imitate the piston bosses and the connecting rod. This will be a simplification of the assembly, but when performed in this manner, the focus is always on the piston pin instead of wrong deformation of the piston pin as a consequence of wrong piston or connecting rod material. When this simplification is under dispute, the author of this paper will clearly highlight this, and justify the outcome of these results.

A way to benchmark this is to import the OEM piston pin to the model, analyse the results and use these results as the upper limit for a new design. As the pin needs to be a solid deformable object in Abaqus, it needs to be assigned a material. By assigning steel 4340 material properties to the piston pin, and measuring displacement and stress level, an optimised piston pin with these common steel properties can be proposed.

Just as the previous Abaqus model, this model needs to be reviewed and validated in order to convince its legitimacy. Because this model uses rigid shell elements the model behaves different than the previous.

A friction coefficient between the piston boss and piston pin is set to 0.4, and between the connecting rod and piston pin to 0.6 (Reddy et al., 1994).

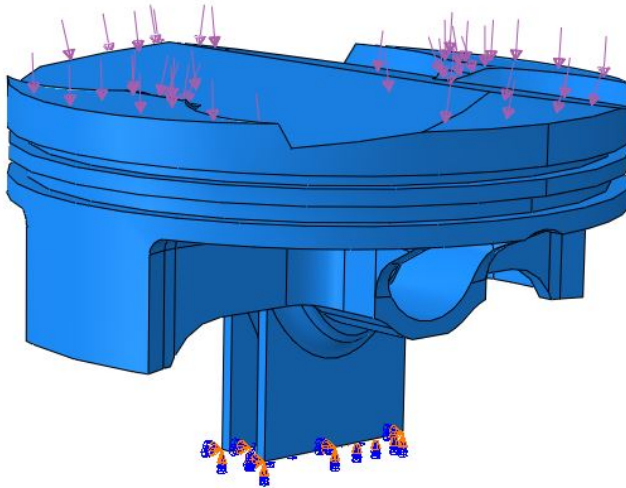


Figure 6.1: Piston assembly

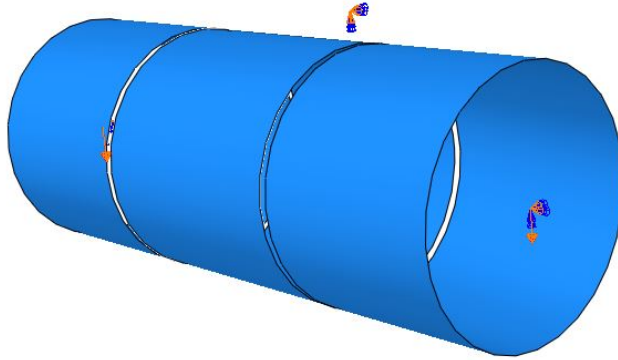


Figure 6.2: The new Abaqus model

6.2.1 Mesh

With this new proposed model, there are a few similarities and a few differences compared with the previous model. For the shell elements the mesh element selection are relatively straight forward and will be in in Abaqus terms as known as R3D4 elements.

From the research for the previous model a discussion regarding the different mesh elements associated with the different challenges has already been presented. The major difference for this model is the pressure force and distribution the non-deformable shell elements will produce on the deformable piston pin.

6.2.2 Mesh Sensitivity Study

A mesh sensitivity study was performed for the model. The study is performed with Von Mises stress against the number of elements used in the analysis. The piston pin used for this analysis was the OEM piston pin. As the results show in figure 6.3, the number of elements needed to perform a reliable analysis is over 70 000. This resulted in the use of element size $0.75mm$ for the further analysis. With the OEM piston pin, this gave a number of elements of 85311. This study is performed with the C3D20R elements.

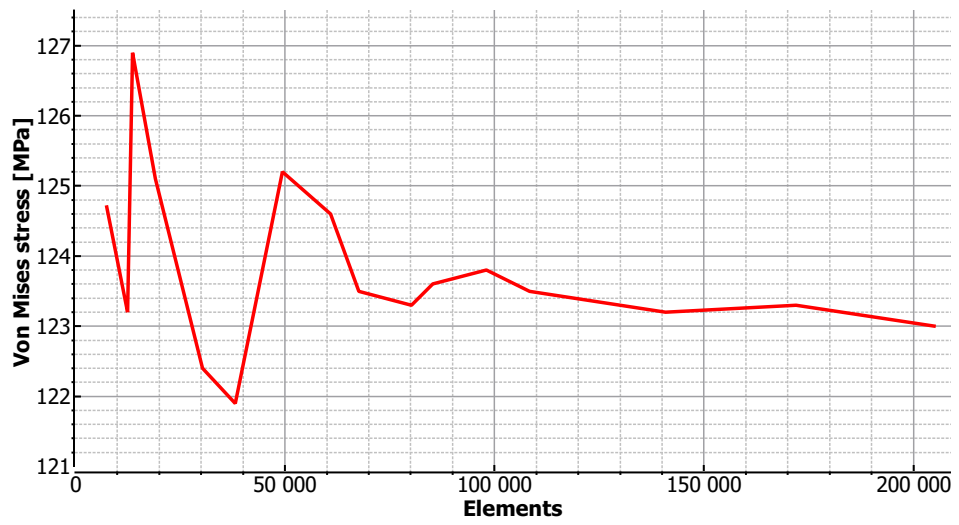


Figure 6.3: Mesh sensitivity study

6.2.3 Geometry

The previous simulation had a $0.02mm$ play (Section 2.2.2) in diameter. This resulted in an elliptical deformation. The Honda crf250r have in theory a fully floating pin. Even so, the clearance between the pin and piston boss are close to zero. The clearance between the pin and connecting rod are about $20\mu m$. Another important aspect is the thermal coefficient, i.e. the thermal expansion of the assembly when the motor heats up. As mentioned, the OEM piston are made out of molded aluminium alloy and the piston pin and connecting rod out of steel. Aluminium have a higher thermal expansion coefficient then steel. Therefore the pin in a Honda CRF250R may be viewed as a crossover between a fully floating pin and a stationary pin. Furthermore, the amount of play in a heated engine between the pin and connecting rod are very small. The amount of difference this can produce is an article done by Ramamurti et al. (2012) and summarized in 3.2. An Abaqus model have been constructed in order to measure the difference this can bring in this analysis. This model is shown in figure 6.4.

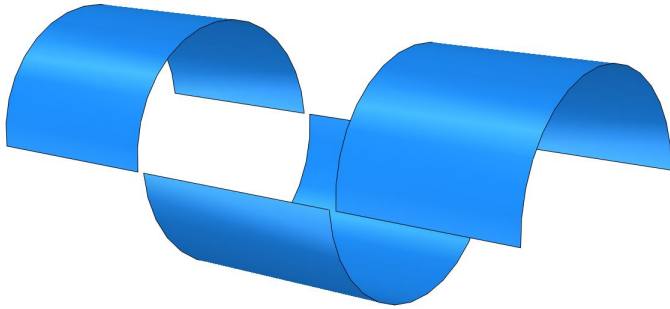


Figure 6.4: Abaqus model for play study

Chapter 7

Optimisation, Results and Discussion

In this chapter, an iterative process to present an optimised piston pin in the common steel material properties is presented. The piston pin is optimised with the material data which corresponds to the 4340 alloy steel. The material properties are shown in table 5.1.

7.1 Path Selection

Abaqus offers a function to use a path along the distance of an object to plot variables including stresses and displacement, for every node in its path. This feature is used in this chapter to display the location and magnitude of the following Von Mises stresses and displacements in the piston pin. The Von Mises path is shown in figure 7.1. As seen, it goes through the point in the pin with peak stress. This method is also used to illustrate the displacement in the pin. Figure 7.2 shows the selection of the displacement paths used and the following numbering of the paths.

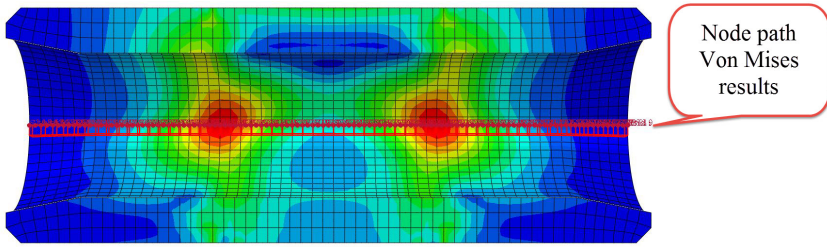


Figure 7.1: Von Mises path OEM

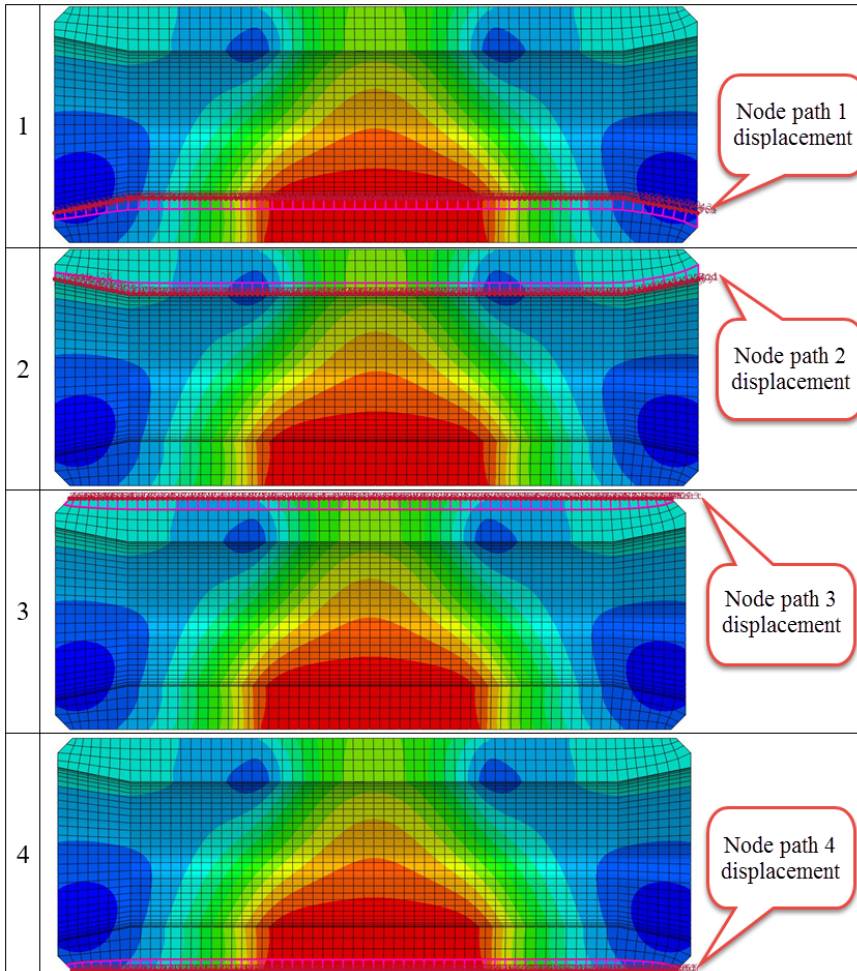


Figure 7.2: OEM displacement paths

7.2 OEM

An analysis of the OEM pin is performed. These results will be the benchmark for a new design. The mass of this pin is $40.147g$. Figure 7.3 and 7.4 shows the results from the Von Mises path and the displacement paths. To illustrate where the location of the results lies, the graph is placed above the post-processing piston pin in Abaqus and the piston boss, connecting rod assembly. The figures show a symmetry along the center of the piston pin in the axial direction for both stress and displacement.

Figure 7.3 show a peak Von Mises stress of $126.8MPa$. With the material properties shown in table 5.1, the OEM piston pin have a factor of safety of 3.71.

A detailed machine drawing of the OEM piston pin is in Appendix B.

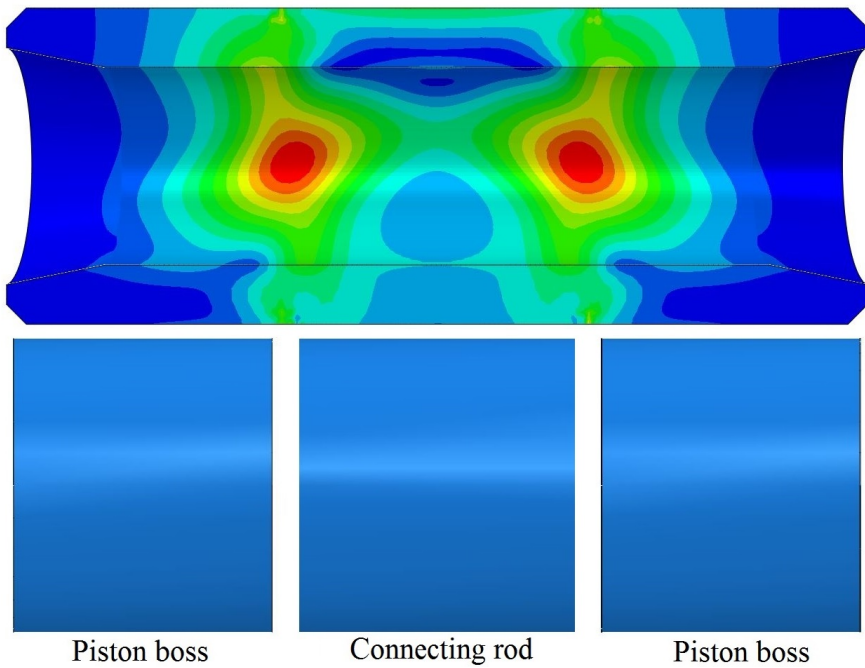
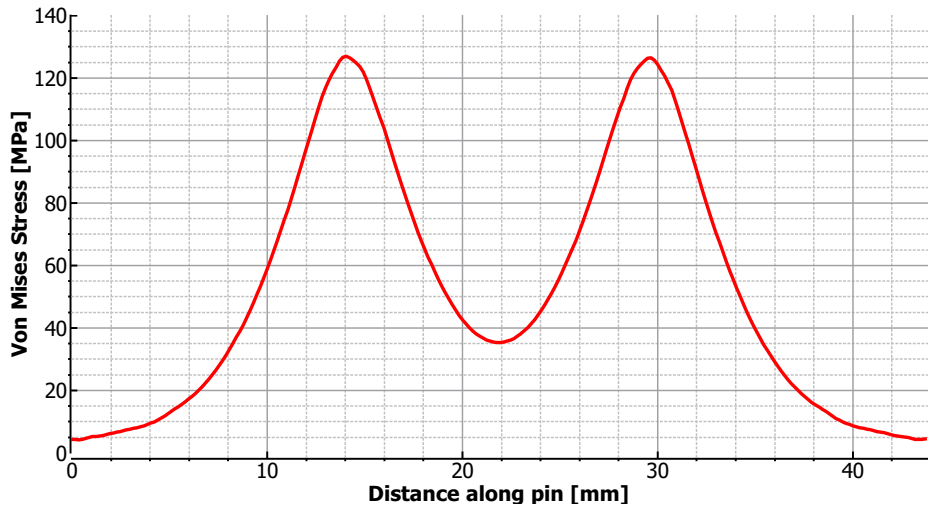


Figure 7.3: Von Mises stress OEM piston pin

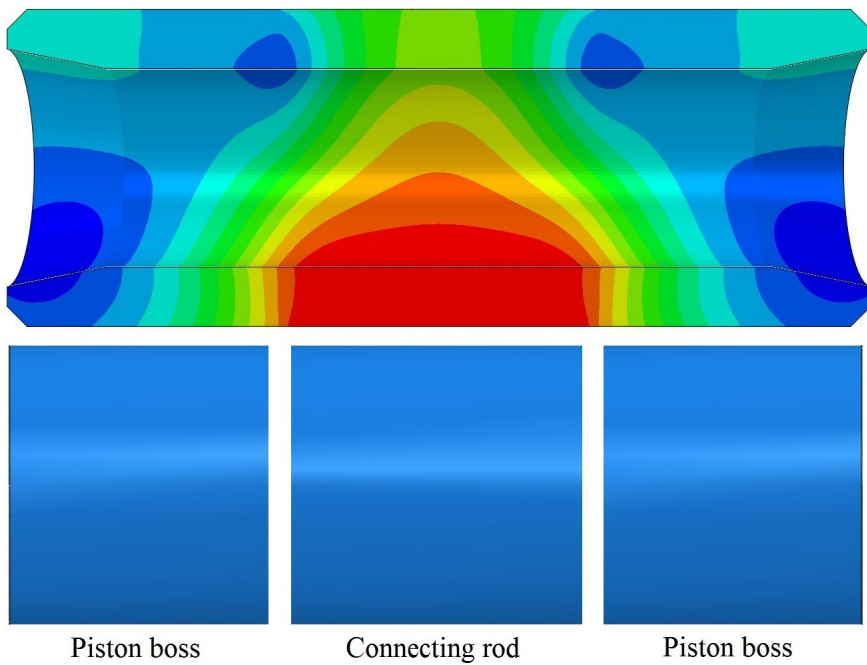
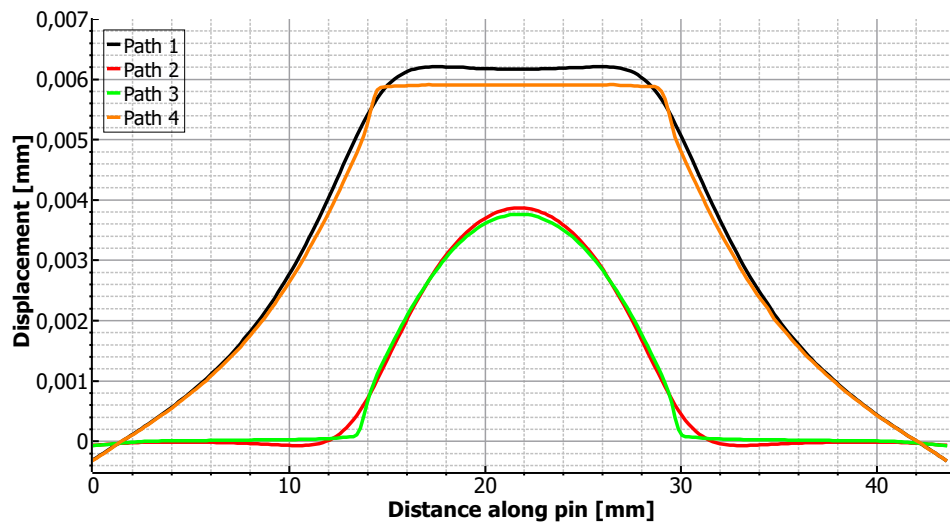


Figure 7.4: Displacement OEM piston pin

7.3 True Hole Piston Pin

In the pin designs proposed by MXRR shown in figure 4.3 they have shortened the length from the OEM at 43.5mm to 41mm . At the beginning of this iteration for the proposal of a new design, this is also done. As talked about in 2.2.1, some piston pin manufactures do not make pins shorter than the length from the piston wall to the piston boss on the opposite side. The piston bore of the Honda CRF250R are 78mm . This means that the length from the cylinder wall to the opposite side is around 46.5mm . Hence this is not practiced by Honda. The limit set by MXRR for the length of the piston pin was 41 mm .

A hollow pin is designed with an inner true hole dimension of 11mm . This is to get a more sensible way to analyse the location and the magnitude in regards to stress and displacement in a pin without an enhancing design. The resulting Von Mises- and displacement paths are shown in figure 7.5 and 7.6. This pin has a mass of 34.125 grams. With this mass reduction and no mechanical design benefits, there is a higher stress and displacement in this piston pin. Maximum Von Mises stress is found 13mm from start (7.5mm from center of the pin) and symmetrical on the other side of the midpoint of the pin, i.e. 28mm from start. This is in the section between the piston boss and the connecting rod, and show the same symmetry as shown in figure 7.3 and 7.4.

The displacement of the pin shows a maximum displacement on the bottom inside of the pin. Maximum displacement occurs along the length of the connecting rod. Displacement path 3 and 4 shows almost half of displacement compared to paths 1 and 2.

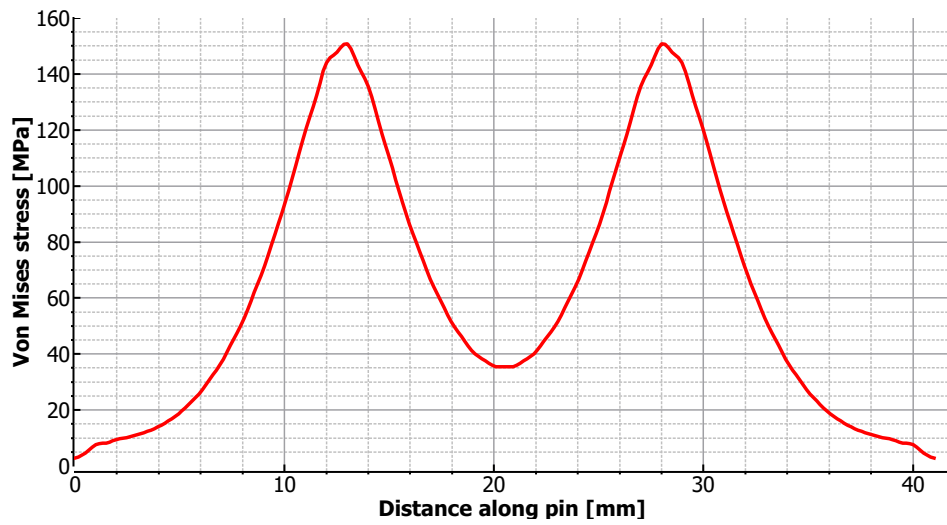


Figure 7.5: Von Mises stress

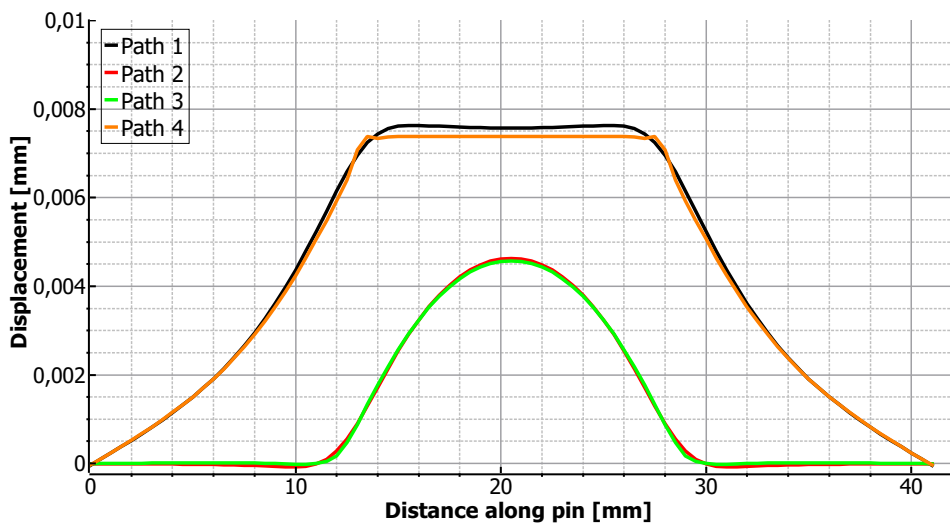


Figure 7.6: Displacement

7.4 Design Proposals

Figure 7.7 shows various designs introduced for further analysing and investigation. As observed, the most stress occur in the section between the piston bosses and the connecting rod. As a result of this, it felt needed to perform analysis of piston designs which contains most material in this section. It can therefore be seen that pin design 1 and 2, 3 and 4 and 5 and 6 have similarity in the meaning of it's geometry. Different geometries is introduced in order to study different advantages and material mass benefits. At this stage, the piston pins proposed are designed with almost equal masses, see figure 7.8, to analyse the geometric advantages they present. The results from the simulation are shown in figure 7.9 and 7.10.

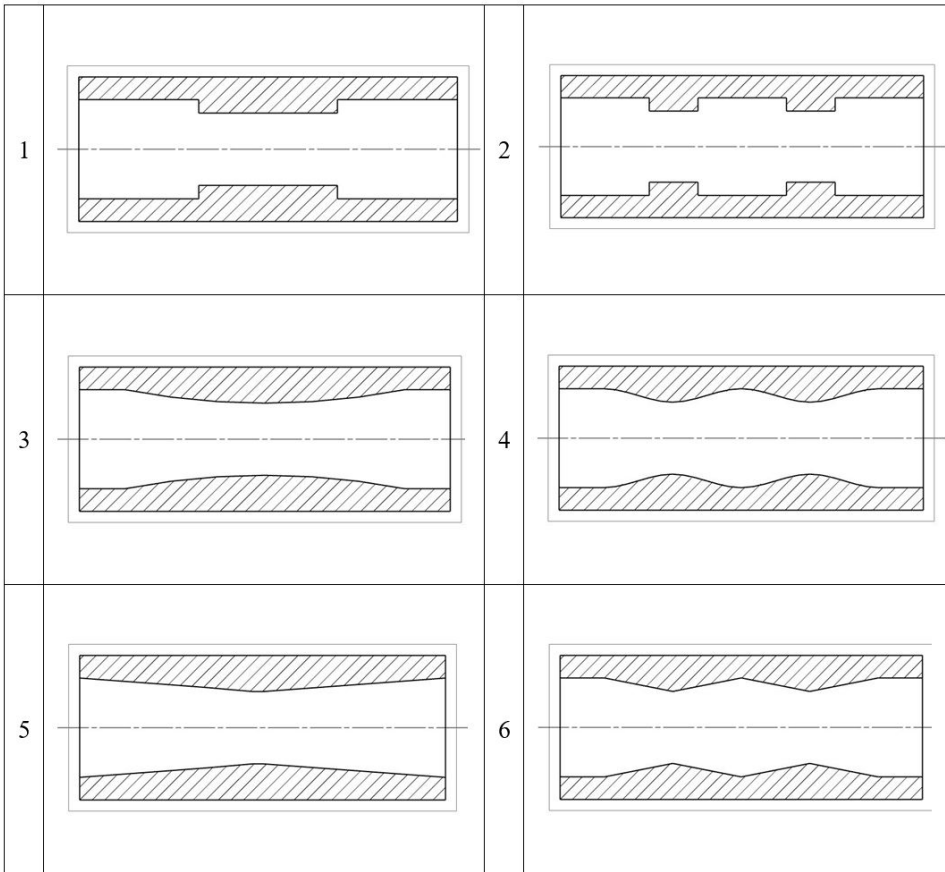


Figure 7.7: Various design proposals

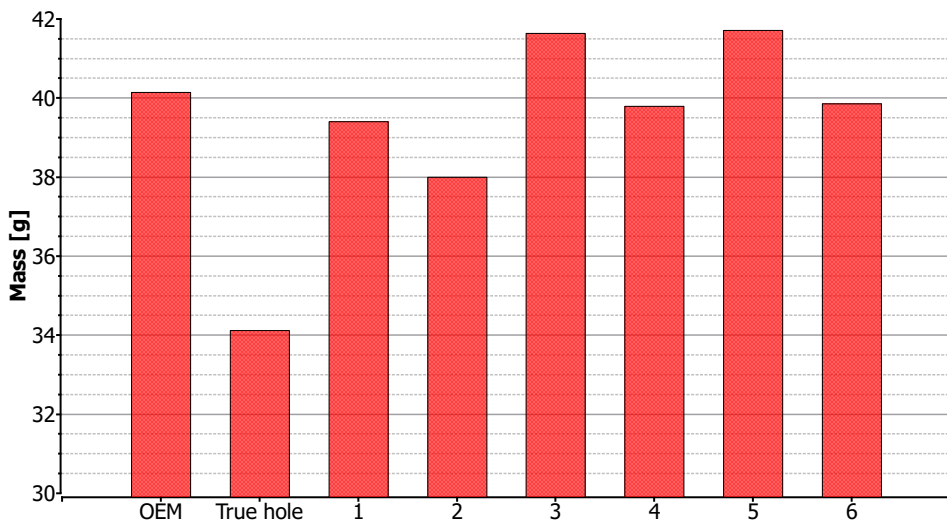


Figure 7.8: Masses

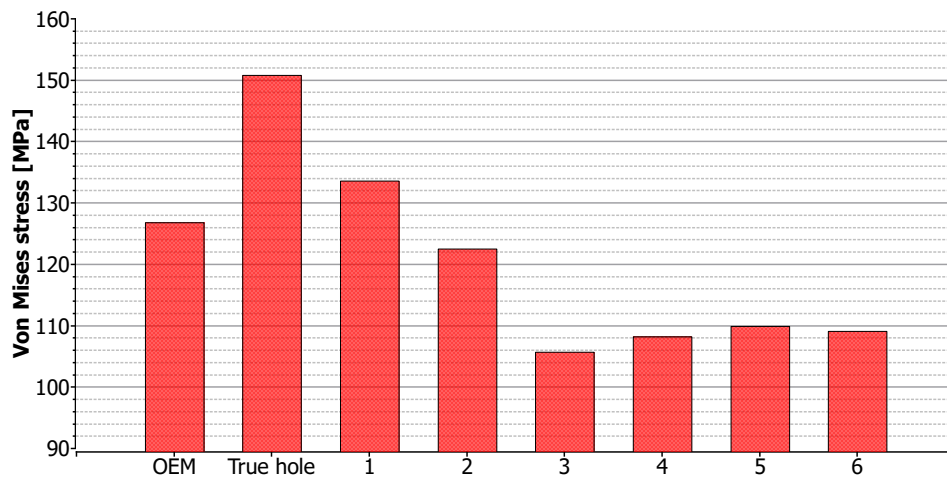


Figure 7.9: Von Mises stress

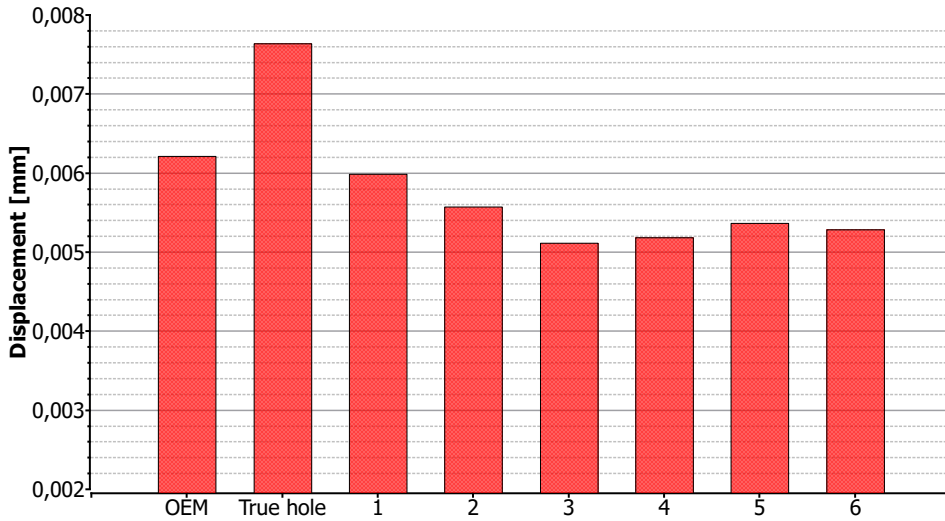


Figure 7.10: Displacement

This iteration is a coarse method in order to separate out the designs that show a weak performance. By studying the results presented, some designs are to be eliminated. Design 1 have a higher mass then its similar designed pin, design 2. In addition to this, pin design 1 also have a higher maximum stress and displacement than pin 2. The same story goes for pin design 5. It has a higher mass than pin design 6, and still a higher stress and displacement. As a result, pin 1 and 5 is not considered in further iterations. The other designs will be further iterated and analysed.

7.5 Further Iteration

In this stage of the process, a closer look at the different geometries is conducted in order to recommend an enhanced proposal of the previous designs. The pins are again designed with almost equal masses in order to measure the geometric advantages presented, figure 7.11.

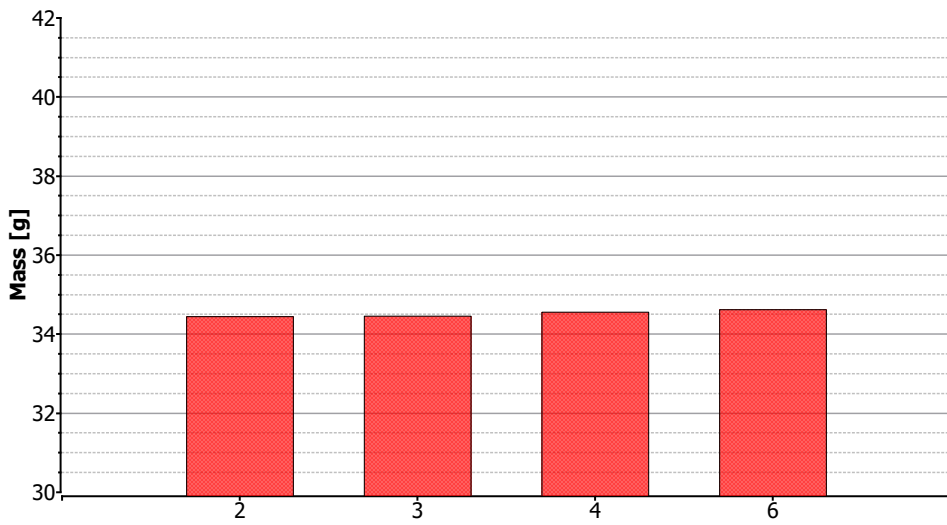


Figure 7.11: Masses

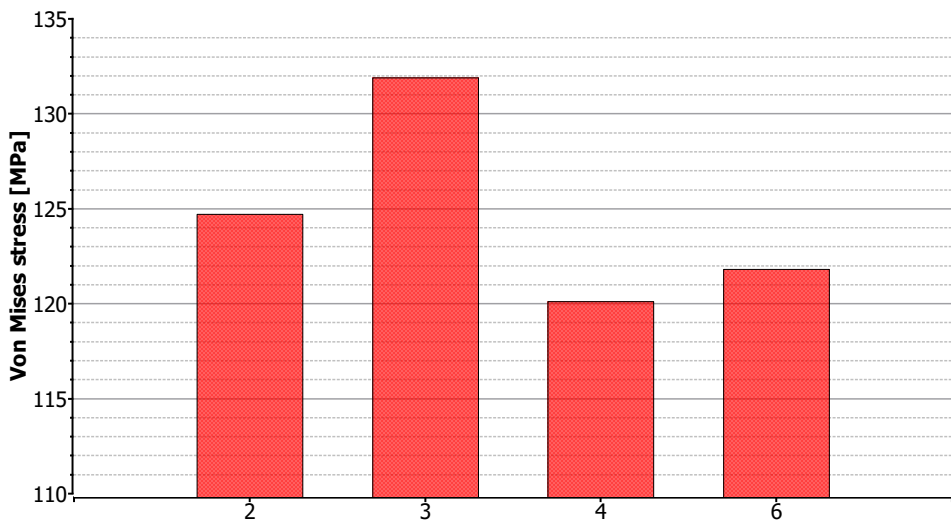


Figure 7.12: Von Mises stress

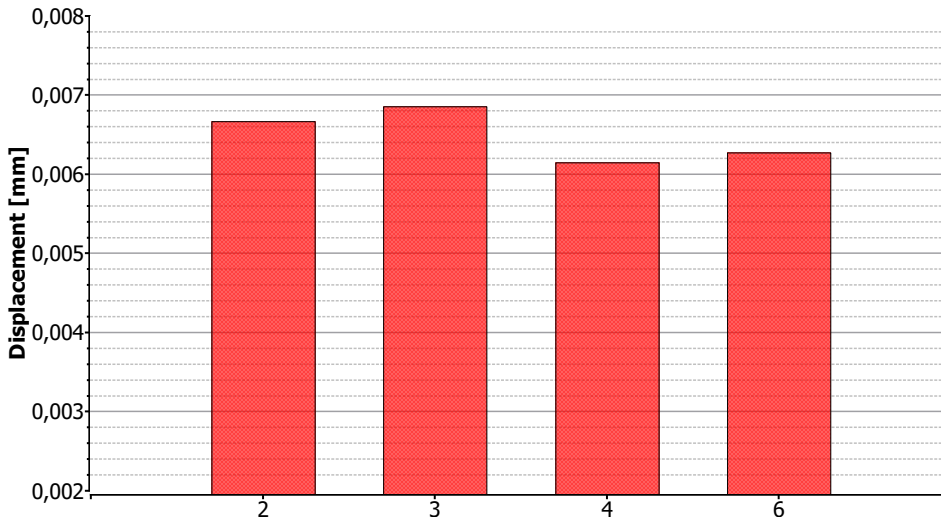


Figure 7.13: Displacement

By analysing the results from this iteration presented in figure 7.12 and 7.13, the pin design that shows the most promise is pin design 4. This has the lowest maximum stress and the lowest maximum displacement. As an extra precaution, the Von Mises stress path is investigated as shown in figure 7.14. This shows an even low stress distribution over all.

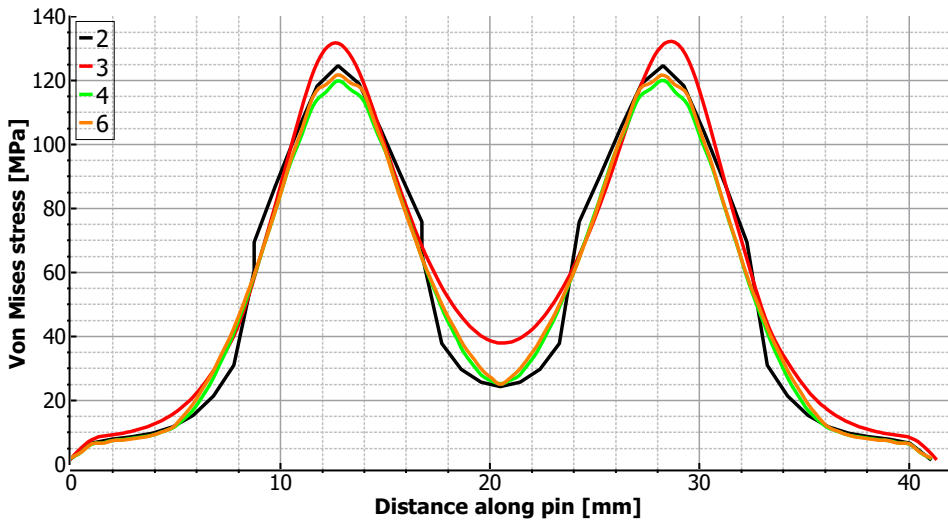


Figure 7.14: Von Mises stress path

7.6 Discussion

Before a final conclusion in regards to the geometric design is taken, a few key points are important to discuss before further iteration will be conducted. The Abaqus model used for the analysis of these results have as mentioned, rigid parts as a consequence of the lack of material information. As seen in the results presented, piston design 2, 4 and 6 generally performed better than its geometrically similar designs. The designs with a better performance are the ones with more mass in the maximum stress region. An evaluation of the validity of this is needed before concluding an optimised design. The result presented show a very stiff construction that exerts the piston pin a high shear stress. The bending depends on the flexibility of the components in the assembly (Fessler and Hyde, 1997). The less flexibility this assembly presents, the lower the bending moment is. The increase of shear stresses depends on the minimization of the length-depth ratio of the pin. As discussed in chapter 3 some consider the piston pin as beams in bending and shear. According to Saint-Venant's Principle (Timoshenko and Goodier, 1951) a sufficient length-depth ratio is needed in order to calculate the piston pin as a simple beam, i.e. simple beam assumes a long beam. The piston pin for this motorcycle do not have a high length-depth ratio and this method will therefore give insufficient result.

As mentioned earlier, the piston is made out of molded aluminium and the connecting rod out of steel. Therefore to verify the results presented, piston pin design 3 and 4 are analysed using the simulation from chapter 5. The displacement from this simulation is shown in figure 7.15. The simulation is done with a modulus of elasticity for aluminium and steel respectively, $79GPa$ and $210GPa$. This can be compared to figure 7.16 which shows the displacement for the simulation with rigid elements. The graphs show similarities and the results show the same conclusion. As a result of this, the premises stated in 7.5 remains as it is.

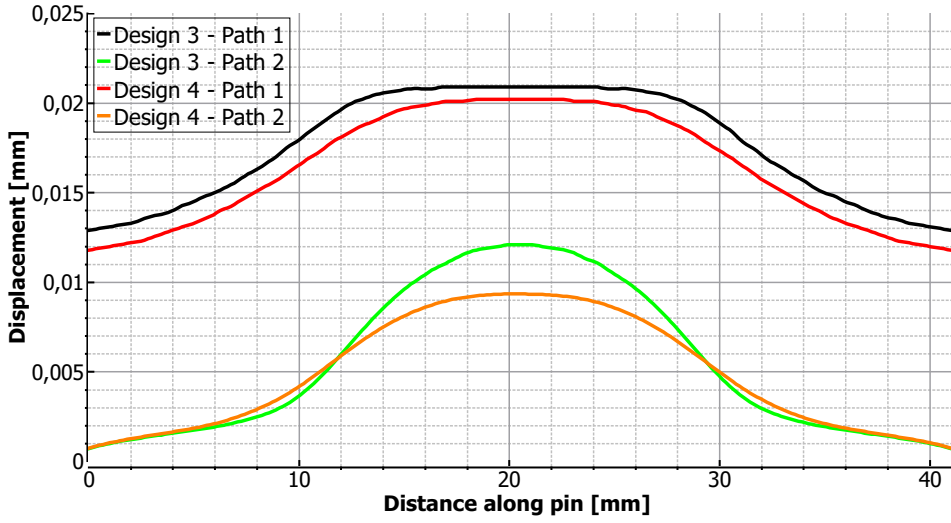


Figure 7.15: Displacement old simulation

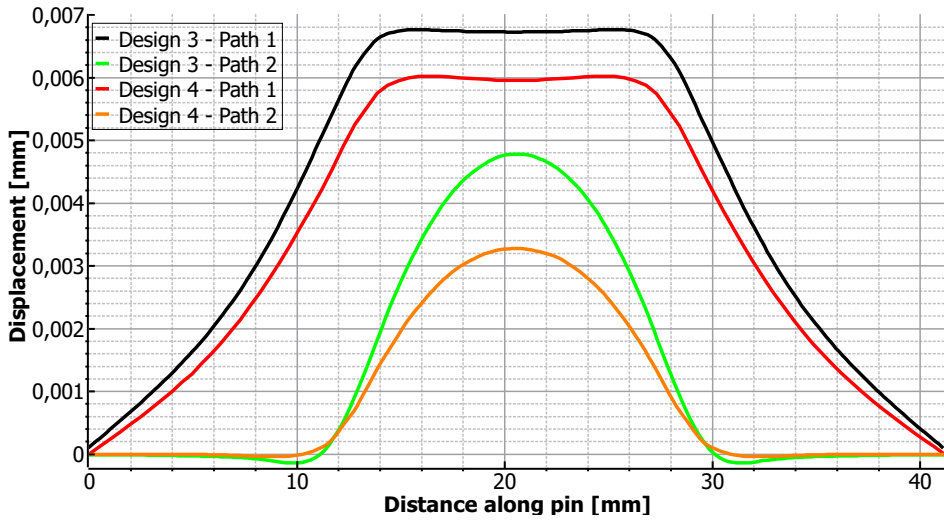


Figure 7.16: Displacement new simulation

7.7 Final Design

At this point, a final geometric design is concluded. But there are still many adjustments that can be made to further optimise the geometric design in order to lower the mass. Figure 7.17 shows 4 different design proposals. Only small adjustments are made in order to investigate exactly where the geometric advantages lies. The numeric numbers given to the respected piston pin designs do not have any relations to the numeric numbers given previously. These variations of the final geometric designs have the force-displacement relations shown in figure 7.18.

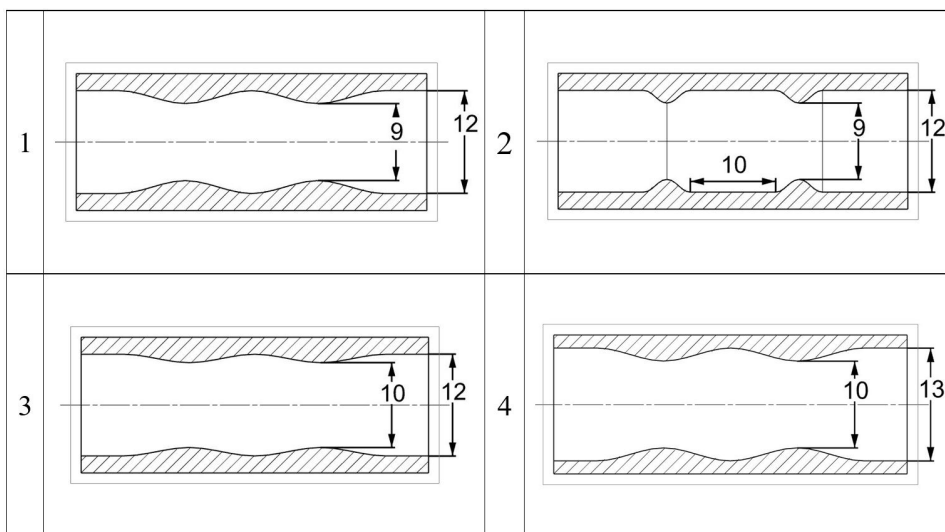


Figure 7.17: Further design proposals

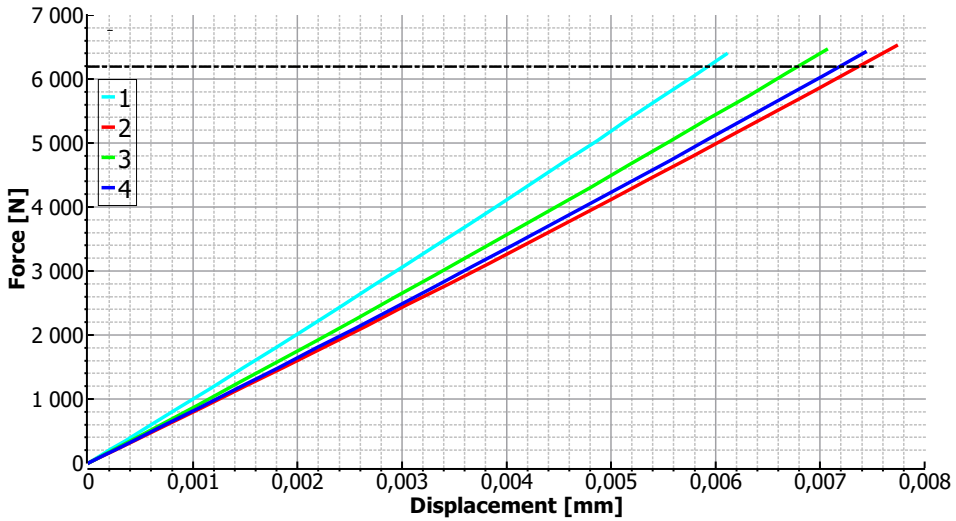


Figure 7.18: Force vs displacement

Piston pin design 1 have the lowest displacement at $6190N$. This design is the same as the previous tested. As a result of this, there is no need to go back and compare results with the previous designs.

From her on now, the design will be iterated in only small adjustment in order to preserve the geometric advantage, but still lower the mass as much as possible. The results of these iteration is benchmarked against the OEM piston pin in order to meet the boundaries given. Figure 7.19 shows the final design. At point A there is a 45 degree angle. This is so it will slide more easily when inserted into the assembly. At point B there is a horizontal wall. This is to protect the piston pin to fracture during installment or removing of the pin e.g. with a hammer (Waldhauer et al., 2004). To save weight, a small slope is designed at point C where the stress is low. A detailed machine drawing is attached in Appendix C. Figure 7.20 and 7.21 show the stress distribution and displacement distribution, respectively, for the final design and OEM piston pin.

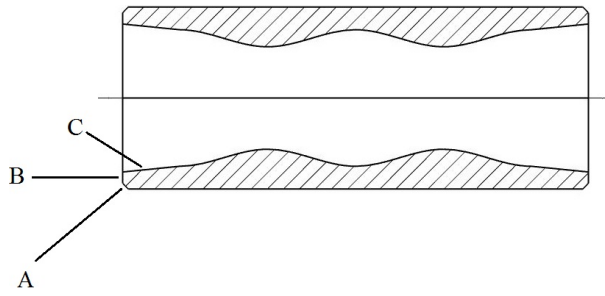


Figure 7.19: Final design

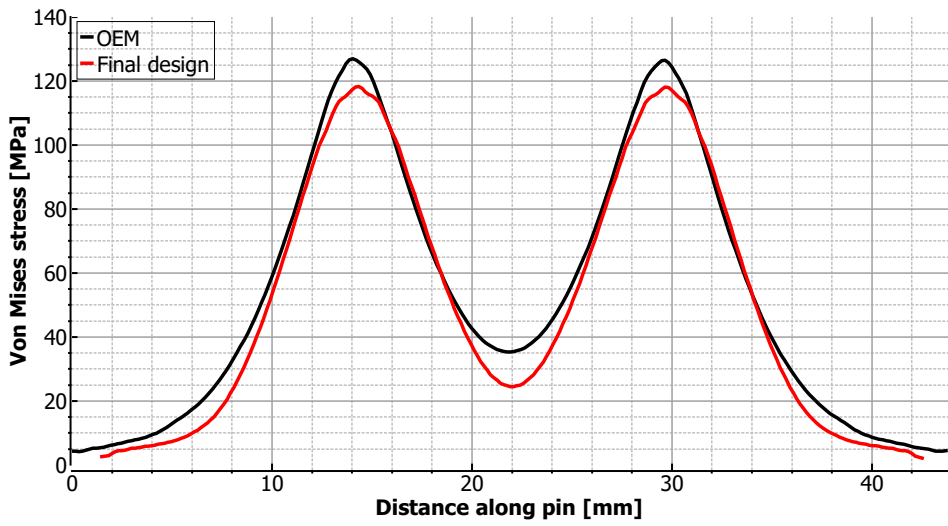


Figure 7.20: Final design stress vs OEM stress

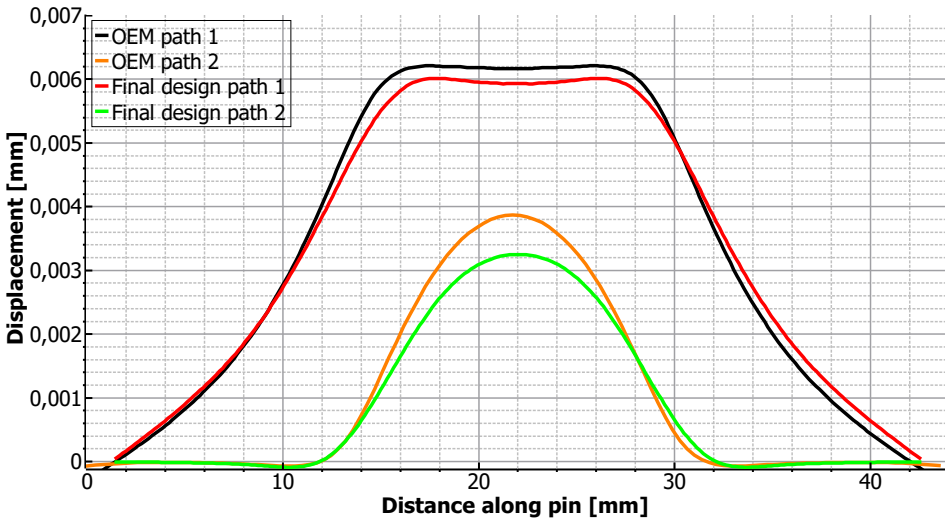


Figure 7.21: Final design displacement vs OEM displacement

The final design mass calculated with a mass density of $7850\text{kg}/\text{m}^3$ is 33.695g . The OEM has a mass of 40.147g with the same mass density. As a result of this there is a mass reduction of 16.07%. The overall stress in the final design is lower than the OEM pin. At peak Von Mises stress for the final design and OEM is respectively 118.3MPa and 126.8MPa . That means a peak stress reduction of 6.7%. The displacement at path 1 and 2 is plotted for the final design and OEM pin in figure 7.21. This shows a reduction for path 1 and 2 at respectively 3.17% and 16.02%. The amount of mass reduced and still stay within the perimeter set, shows the importance of mechanical design.

7.8 Play Analysis

An analysis using the Abaqus model described in section 6.2.3 to examine the difference of play values was carried out. To be sure if the amount of play will change the outcome of the results just presented, an analysis of the final design was benchmarked against the OEM. The results this analysis presented gave the same conclusion, i.e. even with a high amount of play, the final design gives a lower Von Mises stress and displacement than the OEM piston pin.

As presented in 3.2, Ramamurti et al. (2012) describes the difference in stress and displacement if the piston pin touches the piston bore or not (Contact in point A1 and A2 in figure 3.1. A similar analysis is performed for the final design. The result of this gave a maximum Von Mises stress of $124.5MPa$ and a maximum displacement of $0.006493mm$. The Abaqus model without play gave a result of maximum Von Mises stress of $118.3MPa$ and a maximum displacement of $0.006012mm$. This shows that there is a reduction of stress and displacement when the piston pin is in contact with the piston bore. These results is in affiliation with the findings of Ramamurti et al. The maximum deflection of the free end is $0.0004176mm$.

7.9 Machining

The final design have a complex geometry. ISCAR LTD. is the largest of 15 companies comprising the IMC (International Metalworking Companies) (ISCAR LTD., 1952). They provide a wide range of carbide inserts, carbide end mills and cutting tools, covering most metal cutting applications. One of the internal profiling tool they make are the PICCOCUT series. An example of a PICCOCUT tool is shown in figure 7.22a and an illustration of the internal profiling with this tool is shown in figure 7.22b. Iscar provides a wide range of these tools for the profiling application in what they call miniature dimensions. In figure 7.23 are a bundle of different parameters that can be adjusted in order for finding the right tool for an application. An example of a PICCOCUT tool that would be competent for the purpose of profiling the inside of the final design piston pin is found in table 7.1.



Figure 7.22: Iscar tool (a) and sketch of the internal profiling (b). (ISCAR LTD., 2016)

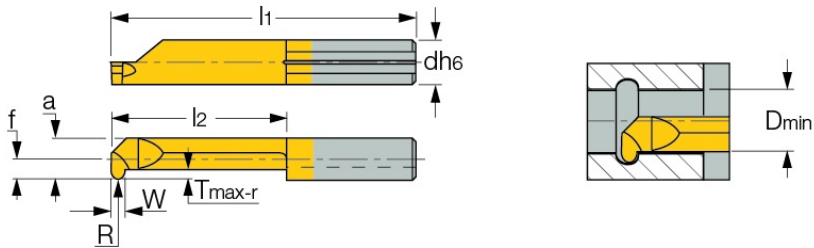


Figure 7.23: Iscar PICCOCUT tool dimensions (ISCAR LTD., 2016)

Table 7.1: Iscar PICCOCUT tool dimensions (ISCAR LTD., 2016)

Designation	d	$W \pm 0.05$	f	a	R	l1	l2	$T_{\max-r}$	D min	Grade
PICCO 006.0.50-25	6.00	1.00	2.3	5.3	0.50	40.00	24.0	1.80	6.00	IC228

Chapter 8

Summary

8.1 Further Work

If an extension of this thesis is conducted, the very first work to be done is to find the error in which the Abaqus analysis and physical test did not behave the same. As mentioned, since the physical testing of the piston pins was outsourced, it was difficult for the author of this paper to locate the inaccuracy or failure that could have happened here.

As for the new simulation that was constructed. This thesis show that a lot can be done regarding optimisation of the piston pin by modifying the design. Since the piston pin experiences a hard and intricate environment, there are many more factors that could be implemented in order to make the analysis more realistic. All of which should include the material properties for every part in the assembly.

The foundation of this thesis is the known parameters of the Honda CRF250R bike and previous work. To give an example, the friction coefficient given to the Abaqus simulation. A way to provide the exact correct coefficient number would be to obtain the material data, gain an overview of the lubrication conditions in the engine and perform tribology tests with the basis of this knowledge (Etsion et al., 2006). Therefore it would benefit the FE analysis with real life testing of conditions given to the piston pin.

A list of physical tests that would benefit the analysis:

- Friction and lubrication conditions.
- The amount of play in the assembly. An important notice would be to measure the dimensions when the parts are cold and when the parts are heated up on the basis of thermal expansion.
- Implement fatigue
- Study and replicate results focused on fracture

These tests are also important to further optimise the piston pin in general. Thus a broader analysis, the more benchmark indicators can be set and the analysis will be more accurate.

Material properties are of course an important factor in further optimising the piston pin. Both physical testing and FE analysis of different materials could benefit further evaluations of appropriate materials to be used. In Appendix A.1, a introduction into various light weight metals with a high strength-weight ratio is presented. Additionally the benefits and challenges with these materials are discussed. In Appendix A.2, a introduction to the ceramic material silicon nitride is presented with a discussion of the benefits and challenges associated with this material.

8.2 Conclusion

The objective set out from the beginning was to identify the optimal combination of piston pin shape and material. The material data would be obtained from iterating the Abaqus analysis to match the physical testing done by MXRR. Due to the misalignment between the Abaqus result presented and the physical testing this objective could not be performed. For this reason, new objectives were introduced.

By obtaining vital information about the parameters of the Honda CRF250R motorcycle piston assembly and attaining a higher knowledge regarding the crank

system and its components, this thesis generated a FE model to test various piston pin designs. By analysing the quasi-static test performed on the OEM piston pin and a piston pin without a mechanical enhancing design, a profound understanding of stresses and displacements are presented. By implementing piston pin designs with the intention of reducing weight but maintaining the desired strength parameters, the benefit of mechanical design optimisation is introduced. The various designs proposed gives an insight into how the different designs performs under the given load and boundary condition parameters. An optimised piston pin with a lower mass is the result of the iteration process executed. The mass of the optimised piston pin is 33.695g. This is a reduction of 16.07% from the OEM piston pin.

Bibliography

- Abed, G., Zou, Q., Barber, G., Zhou, B., Wang, Y., Liu, Y., and Shi, F. (2013). Study of the motion of floating piston pin against pin bore. *SAE International Journal of Engines*, 6(2013-01-1215):990–998.
- Budinski, K. G. (1991). Tribological properties of titanium alloys. *Wear*, 151(2):203–217.
- Chen, K., Zhou, Y., Li, X., Zhang, Q., Wang, L., and Wang, S. (2015). Investigation on wear characteristics of a titanium alloy/steel tribo-pair. *Materials & Design*, 65:65–73.
- Dassault Systèmes (2013). Getting started with abaqus: Interactive edition 6.13. <http://orange.engr.ucdavis.edu:2080/v6.11/books/gsa/default.htm?startat=ch02.html>. Accessed: 30-05-2016.
- Dassault Systèmes (2014). Getting started with abaqus: Keywords edition 6.14. <http://ivt-abaqusdoc.ivt.ntnu.no:2080/v6.14/books/gsk/default.htm?startat=ch13.html>. Accessed: 30-05-2016.
- Dixon, J. (1960). A photoelastic examination of the stress distribution in gudgeon pins. *NEL report MCZH/JRD/PE2*, 16:3.
- Etsion, I., Halperin, G., and Becker, E. (2006). The effect of various surface treatments on piston pin scuffing resistance. *Wear*, 261(7):785–791.
- Fessler, H. and Hyde, T. (1997). Stress distribution in gudgeon pins. *The Journal of Strain Analysis for Engineering Design*, 32(5):375–386.

- Fessler, H. and Padgham, H. (1966). A contribution to the stress analysis of piston pins. *The Journal of Strain Analysis for Engineering Design*, 1(5):422–428.
- Froes, F., Friedrich, H., Kiese, J., and Bergoint, D. (2004). Titanium in the family automobile: the cost challenge. *Jom*, 56(2):40–44.
- Giannone, M. (2016). Mgp connecting rods. <http://www.dragracingscene.com/tech-content/keep-pin-spinning/>. accessed: 23-05-2016.
- Gupta, R., Kumar, V. A., and Chhangani, S. (2016). Study on variants of solution treatment and aging cycle of titanium alloy ti6al4v. *Journal of Materials Engineering and Performance*, 25(4):1492–1501.
- Heiserman, D. L. (2015). Editor waybuilder. <http://www.waybuilder.net/freed/Courses/15%20Transportation/AutoTruck03/AutoTruckShow.asp?iNum=010102>. Accessed: 2016-09-05.
- Hoffmann, M. J. and Petzow, G. (2012). *Tailoring of mechanical properties of Si₃N₄ Ceramics*, volume 276. Springer Science & Business Media.
- ISCAR LTD. (1952). Iscar ltd. <http://www.iscar.com/products.aspx/countryId/1/productid/39>. Accessed: 2016-23-05.
- ISCAR LTD. (2016). Iscar ltd. <http://www.iscar.com/products.aspx/countryId/1/productid/39>. Accessed: 2016-23-05.
- Ji, B., Li, J., and Chen, X. (2012). Research on piston pin’s strength calculation based on fea. In *Advanced Materials Research*, volume 341, pages 296–300. Trans Tech Publ.
- May, U., Stromberger, F., Kohl, J., Berroth, K., et al. (2008). Technology potential of ceramic piston pins. *MTZ worldwide*, 69(5):46–51.
- Piston (2016). Piston pins and piston pin circlips. In *Cylinder components: Properties, applications, materials*, pages 25–46. Springer Fachmedien Wiesbaden, Wiesbaden.

- Ramamurti, V., Sridhar, S., Mithun, S., Kumaravel, B., and Lavanya, S. (2012). Design considerations of gudgeon pin in reciprocating air compressors by semi analytic approach. *Journal of Mechanical Engineering Research*, 4(3):75–88.
- Reddy, A. S., Bai, B. P., Murthy, K., and Biswas, S. (1994). Wear and seizure of binary al? si alloys. *Wear*, 171(1):115–127.
- Rothmann, G. (1963). Berechnung der kolbenbolzen von fahrzeugdiesel-motoren. *Mitteilungen aus den Forschungsanstalten von GHH Konzern*, 4:231–238.
- Schlaefke, K. (1940). Zur berechnung von kolbenbolzen. *Molortechnische Zeitschrift*, 2:117–120.
- Shi, F. (2011). An analysis of floating piston pin (2011-01-1407). *SAE International Journal of Engines*, 4(1):2100.
- Siemens PLM Software Inc. (2016). About nx software. https://www.plm.automation.siemens.com/en_us/products/nx/index.shtml. Accessed: 30-05-2016.
- Timoshenko, S. and Goodier, J. (1951). *Theory of Elasticity*. McGraw-Hill book Company.
- Waldhauer, B., Schilling, U., Schnaibel, S., and Szopa, J. (2004). *Piston damage*. MSI Motor Service International GmbH, Neckarsulm, Germany.
- Wang, Y. and Gao, H. (2011). Research on optimization for the piston pin and the piston pin boss. *Open Mechanical Engineering Journal*, 5:186–193.
- WordPress (2015). What is a four stroke combustion cycle. <http://importautorepairindy.com/blog/what-is-a-four-stroke-combustion-cycle/>. Accessed: 2016-09-05.

Appendix A

A.1 Light Weight Metals

An important aspect in reducing weight in the high performance industry is the advantage of using lightweight materials such as aluminium, magnesium and titanium. Not only do they have a high strength-to-density ratio but their corrosion resistance gives another important benefit. The advantages of this is not exactly ground-breaking news. Both Daimler and Benz made their engines out of aluminium at the end of the 1800s and the start of the 1900s. Even the Wright brothers made their first successful heavier-than-air powered aircraft with an aluminium engine block just for the reason to save weight. Aluminium was considered as a soft metal, but the recent developments of alloys showed promise with a higher strength. And it is here the industry strives. With a goal in the horizon with the lightest material with the strength of steel, the continuous improvements of alloys and further post production enhancements of the material properties will always be a research with a high potential.

Even titanium isn't relatively new in the use of the engine. Already in the mid 1950s General Motors manufactured the Firebird II with an outer skin of titanium. For the use of a vital engine part, the titanium can be dated to at least 1992 when Honda used it for the connecting rod in their NSX model (Froes et al., 2004). Because of the cost of titanium metal, the only users are perfectionist amateurs and the high performance industry. The advantage of lightweight metals, not only

for performance, but also for lower emissions and lower fuel consumption, the use of these metals in the everyday family car is just too expensive.

Even though there are a lot of advantages of the material properties in these metals, a main concern is the wear of the metal. For the example of titanium alloys, they show a poor wear tribological properties (Budinski, 1991; Chen et al., 2015). Because of this the connecting rod and piston pin cannot be a steel and titanium coupling because of abrasive- and fretting wear. One way to solve this is to use or change the connecting rod bushing to another material with a lower wear property against titanium.

Another way to reduce wear problem is by DLC (diamond-like carbon) coating. DLC coating is a nanocomposite coating with unique properties of natural diamond such as low friction, high hardness, high corrosion resistance and a high wear resistance.

Because an optimised piston pin is a more concern for racing than the family car the cost are a less concern. This has led to a number of production companies making piston pins in these light weight metals. With a mass density of $4430\text{kg}/\text{m}^3$, a change from steel to titanium piston pin, a high mass reduction is expected. Since titanium has a lower modulus of elasticity then steel (approximately 114GPa vs 210GPa), a direct switch from a steel pin to a titanium pin without a change in design will lead to a lower factor of safety. With the wear problem at an acceptable level and a carefully considerations of the factor of safety, there is no reason for why a change from steel piston pin to a more light weight metal cannot be done.

A special note can also be made of very exotic piston pins whereas industry such as Formula One use two different materials to make a composite piston pin. Examples of this is an aluminium beryllium inner core and steel outer sleeve.

A.2 Ceramics

In recent years, the considerations of ceramic materials for the piston pin have been introduced. More specified, the ceramic material silicon nitride with the chemical formula, Si_3N_4 . Silicon nitride have proven quite suitable in regards to weight, strength, temperature resistance, friction and wear (Hoffmann and Petzow, 2012). The material have already shown great promise in the automobile industry. Because of its material properties, silicon nitride have already found its way into parts such as: glowplugs, turbochargers, rocker arms and the intake and exhaust valves.

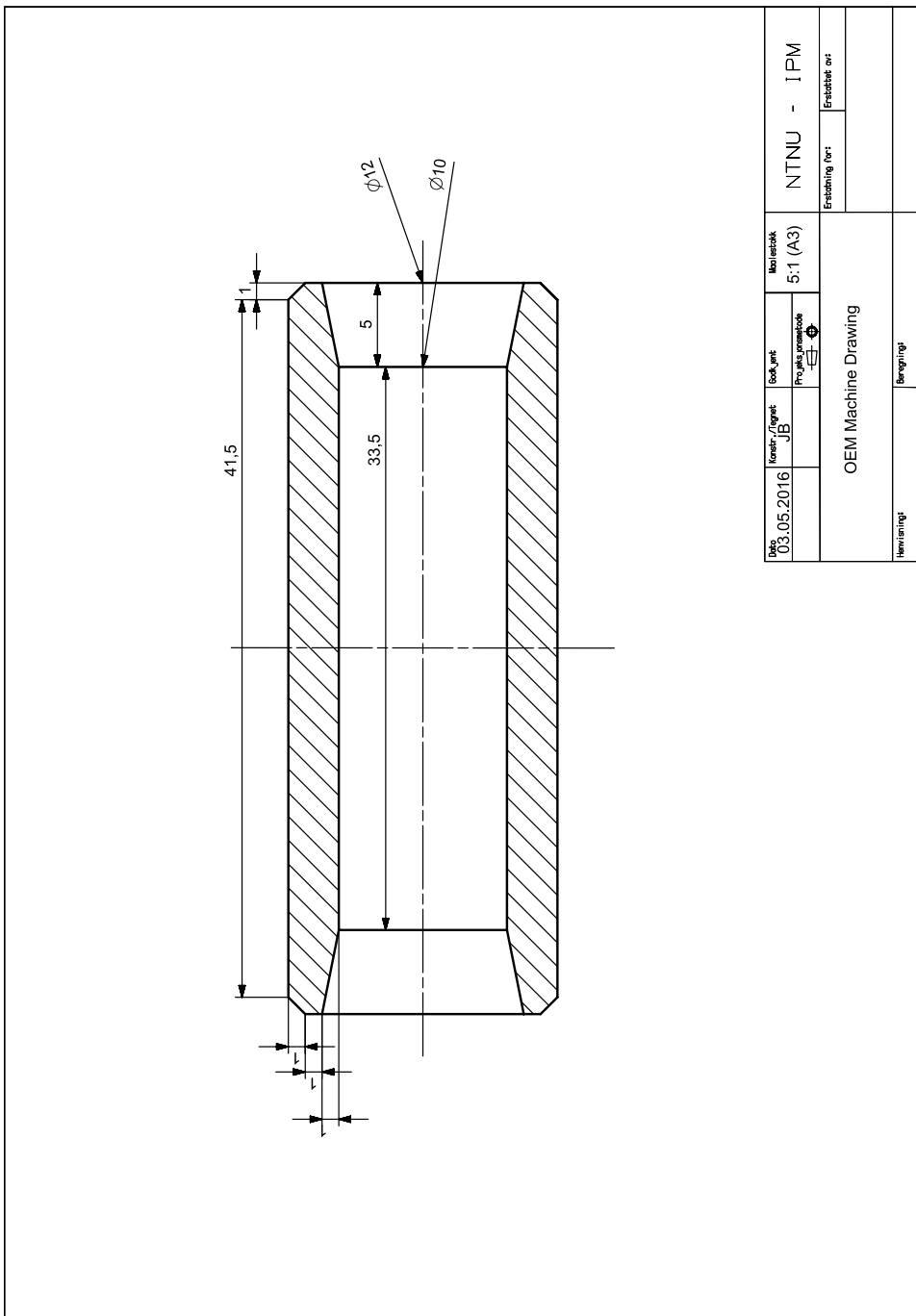
A challenge featured with silicon nitride is the production and processing. After the silicon powder is heated up and further formed, the body is ready for machining. This is done under the phase called green machining. This is when the ceramic have not been sintered yet. In this stage the machining will remove most of the mass of the component. The coarse machining is done in this stage because after sintering, the ceramic becomes so hard and dense that only a minimum amount of grinding and shaping is possible. During the sintering the high temperature fuse the ceramic particles together and the part will experience a shrinkage of about 20%. An important aspect for the success of this is to accurate a prediction of this shrinkage. After the final sintering the part can be machined with diamond tools or laser processing to the right dimensions.

An article done by May et al. (2008) researched the potential of the silicon nitride ceramic piston pins. It further discuss the production and processing stage and performed a durability test on a piston pin. In addition, a study of the tribology of the silicon nitride is carried out. The summary and outlook of the article concludes that for the basis under their research, a silicon nitride piston pin are the preferred material.

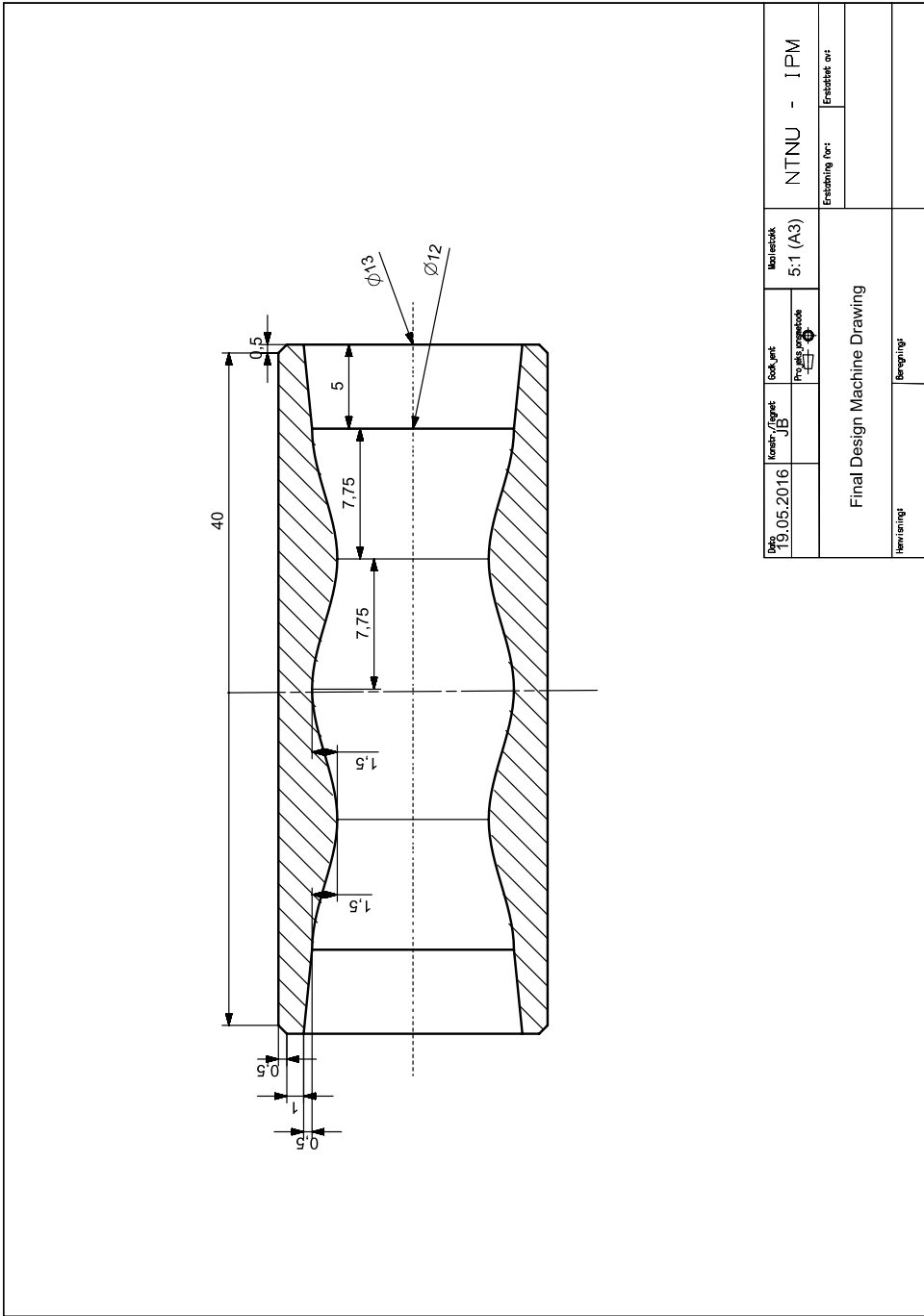
Just as the light weight metals, ceramic is more expensive then steel. Because of this ceramic piston pins is more likely to implement in the racing industry then the everyday car. Due to the uncertainty of the reliability of the ceramic components, research in this field starts with components that will not lead to total engine

failure if the ceramic part is to fail. Now that important parts such as the valve show great promise, it is only a matter of time before the research of the piston pin will gain more interest. Since the racing industry is a competitive industry, research in this field may have come far, but not much information is out there in regards to the implementation of the ceramic piston pin. The information that do exist show a lot of promise when compared to materials used today.

Appendix B



Appendix C



Appendix D

THE NORWEGIAN UNIVERSITY
OF SCIENCE AND TECHNOLOGY
DEPARTMENT OF ENGINEERING DESIGN
AND MATERIALS

MASTER THESIS AUTUMN 2015 FOR STUD. TECHN. JOAKIM BØHN

PISTON PIN TESTING

Piston pin testing

Most modern engines use some form of forged steel connecting rod and piston pin for its balance of strength, durability, and weight. However, most designs leave much room for improvement of materials, design and manufacturing.

MXRR has introduced state of art titanium connecting rods and is currently doing physical testing of piston pins in various designs and materials. NTNU wants to use these test results to create and validate FE models and virtual test procedures that reproduce the physical tests. The objective is to establish virtual tests setups and material models that can be used to optimize future piston pin designs

Tasks to be completed are:

1. Study and document the physical tests performed by MXRR. Identify the piston pins and test results to be virtually benchmarked. Define test requirements
2. Create CAD and FE models of the test rig and selected piston pins in NX
3. Perform quasi static crash tests (Abaqus or NX SOL 601/701) of the piston pins and document the applied reaction forces until pin failure.
4. Tune the materials and FE models until virtual and physical test results match
5. Identify piston pins and materials with optimal "strength to weight ratio"
6. Prepare a paper together with MXRR and the supervisor

Formal requirements:

Three weeks after start of the thesis work, an A3 sheet illustrating the work is to be handed in. A template for this presentation is available on the IPM's web site under the menu "Masteroppgave" (<http://www.ntnu.no/ipm/masteroppgave>). This sheet should be updated one week before the master's thesis is submitted.

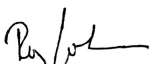
Appendix D

Risk assessment of experimental activities shall always be performed. Experimental work defined in the problem description shall be planned and risk assessed up-front and within 3 weeks after receiving the problem text. Any specific experimental activities which are not properly covered by the general risk assessment shall be particularly assessed before performing the experimental work. Risk assessments should be signed by the supervisor and copies shall be included in the appendix of the thesis.


The thesis should include the signed problem text, and be written as a research report with summary both in English and Norwegian, conclusion, literature references, table of contents, etc. During preparation of the text, the candidate should make efforts to create a well arranged and well written report. To ease the evaluation of the thesis, it is important to cross-reference text, tables and figures. For evaluation of the work a thorough discussion of results is appreciated.

The thesis shall be submitted electronically via DAIM, NTNU's system for Digital Archiving and Submission of Master's theses.

The contact person is Matteo Bella from MXRR.


for Torgeir Welø
Head of Division


Terje Rølvåg
Professor/Supervisor

 NTNU
Norges teknisk-
naturvitenskapelige universitet
Institutt for produktutvikling
og materialer

